Regional uplift associated with continental large igneous provinces: The roles of mantle plumes and the lithosphere

A.D. Saunders [a],*, S.M. Jones [b], L.A. Morgan [c], K.L. Pierce [d],
M. Widdowson [e], Y.G. Xu [f]

[a] Department of Geology, University of Leicester, Leicester LE1 7RH, United Kingdom
[b] Department of Geology, Trinity College, Dublin 2, Ireland
[c] U.S. Geological Survey, MS 966, Box 25046, Federal Center, Lakewood, CO 80225, USA
[d] U.S. Geological Survey, Northern Rocky Mountain Science Center, P.O. Box 173492, Bozeman, MT 59717–3492, USA
[e] Department of Earth Sciences, The Open University, Walton Hall, Milton Keynes, MK7 6AA, United Kingdom
[f] Key Laboratory of Isotope Geochronology and Geochemistry, Guangzhou Institute of Geochemistry,
Chinese Academy of Sciences, P.O. Box 1131, 510640 Wushan Guangzhou, PR China

Abstract

The timing and duration of surface uplift associated with large igneous provinces provide important constraints on mantle convection processes. Here we review geological indicators of surface uplift associated with five continent-based magmatic provinces: Emeishan Traps (260 million years ago: Ma), Siberian Traps (251 Ma), Deccan Traps (65 Ma), North Atlantic (Phase 1, 61 Ma and Phase 2, 55 Ma), and Yellowstone (16 Ma to recent). All five magmatic provinces were associated with surface uplift. Surface uplift can be measured directly from sedimentary indicators of sea-level in the North Atlantic and from geomorpholocial indicators of relative uplift and tilting in Yellowstone. In the other provinces, surface uplift is inferred from the record of erosion. In the Deccan, North Atlantic and Emeishan provinces, transient uplift that results from variations in thermal structure of the lithosphere and underlying mantle can be distinguished from permanent uplift that results from the extraction and emplacement of magma. Transient surface uplift is more useful in constraining mantle convection since models of melt generation and emplacement are not required for its interpretation. Observations of the spatial and temporal relationships between surface uplift, rifting and magmatism are also important in constraining models of LIP formation. Onset of surface uplift preceded magmatism in all five of the provinces. Biostratigraphic constraints on timing of uplift and erosion are best for the North Atlantic and Emeishan Provinces, where the time interval between significant uplift and first magmatism is less than 1 million years and 2.5 million years respectively. Rifting post-dates the earliest magmatism in the case of the North Atlantic Phase 1 and possibly in the case of Siberia. The relative age of onset of offshore rifting is not well constrained for the Deccan and the importance of rifting in controlling magmatism is disputed in the Emeishan and Yellowstone Provinces. In these examples, rifting is not a requirement for onset of LIP magmatism but melting rates are significantly increased when rifting occurs.

Models that attempt to explain emplacement of these five LIPs without hot mantle supplied by mantle plumes often have difficulties in explaining the observations of surface uplift, rifting and magmatism. For example, small-scale convection related to craton or rift boundaries (edge-driven convection) cannot easily explain widespread (1000 km scale) transient surface uplift (Emeishan, Deccan, North Atlantic), and upper mantle convection initiated by differential incubation beneath cratons (the hotcell

---

* Corresponding author. Tel.: +44 116 2523923.
E-mail addresses: ads@le.ac.uk (A.D. Saunders), stephen.jones@tcd.ie (S.M. Jones), lmorgan@usgs.gov (L.A. Morgan), kpierce@usgs.gov (K.L. Pierce), m.widdowson@open.ac.uk (M. Widdowson), yigangxu@gig.ac.cn (Y.G. Xu).

model) is at odds with rapid onset of surface uplift (Emeishan, North Atlantic). The start-up plume concept is still the most parsimonious way of explaining the observations presented here. However, observations of surface uplift cannot directly constrain the depth of origin of the hot mantle in a plume head. The short time interval between onset of transient surface uplift and magmatism in the North Atlantic and Emeishan means that the associated starting plume heads were probably not large (∼ 1000 km diameter) roughly spherical diapirs and are likely to have formed narrow (∼ 100 km radius) upwelling jets, with hot mantle then spreading rapidly outward within the asthenosphere. In cases where rifting post-dates magmatism (N Atlantic Phase 1) or where the degree of lithospheric extension may not have been great (Siberia), a secondary mechanism of lithospheric thinning, such as gravitational instability or delamination of the lower lithosphere, may be required to allow hot mantle to decompress sufficiently to explain the observed volume of magma with a shallow melting geochemical signature. Any such additional thinning mechanisms are probably a direct consequence of plume head emplacement.

1. Introduction

The emplacement of a large igneous province (LIP) on a continent or along a rifting continental margin is an event of major regional and sometimes global significance. In order to understand the mantle processes responsible for the genesis of LIPs, it is important to interpret the igneous record jointly with other observations. The inter-relationships between sedimentation or erosion, tectonics and magmatism are in most cases the only evidence available for constraining the genesis of ancient LIPs, besides the volume, age and composition of the igneous rocks themselves. Here, we are particularly concerned with evidence for changes in surface elevation related to LIP emplacement. Some changes in surface elevation result from addition of igneous rock to the crust. Other changes in elevation reflect changes in the convective structure of the upper mantle and the thermal structure of the plate and asthenosphere. If these latter vertical motions can be recognised and quantified, they can be used to constrain models for LIP genesis. A wide variety of geological observations could be useful in this regard, since changes in surface elevation lead to erosion and affect drainage and sedimentation patterns.

The idea that mantle plumes are responsible for topographic swells up to 2 km in elevation and many hundreds to a few thousand kilometres in diameter is well documented (Morgan, 1971; Burke and Wilson, 1972; Watts, 1976; Crough, 1978; Courtney and White, 1986; McNutt and Judge, 1990; Griffiths and Campbell, 1991; Farnetani and Richards, 1994; Şengör, 2001; Camp and Ross, 2004; Jones and White, 2003). Indeed, Şengör (2001) has suggested that the most unequivocal manifestation of a mantle plume is domal uplift of the Earth's surface. The argument that some modern hotspot swells are predominantly supported by mantle convection derives from the relationship between swell topography and gravity. Since the elastic thickness of oceanic and continental lithosphere does not exceed 50 km (McKenzie and Fairhead, 1997; Watts, 2001; McKenzie, 2003), swells over 700 km in diameter cannot be supported by lithospheric flexure (Turcotte and Schubert, 2002). When regional swell topography is directly proportional to the regional free-air gravity anomaly, the swell cannot be isostatically compensated within the plate, for example by long-wavelength crustal thickness variations, and must be supported by the mantle beneath the plate (Anderson et al., 1973). Since the asthenosphere is the weakest part of the mantle, the low density material supporting the swell must be continually replenished by convection or the swell would quickly deflate (Vogt, 1983). Examples of modern hotspots associated with wide topographic swells and corresponding gravity anomalies are Iceland and Hawaii.

Although gravity data are not available for ancient LIPs, the influence of mantle convection can be still inferred if transient vertical surface motions over large spatial scales and on time scales similar to LIP emplacement (<10 million years: m.y.) can be demonstrated. Mantle plumes are predicted to cause transient surface uplift by several processes. The ascending mantle plume should cause dynamic uplift of the overlying lithosphere (Courtney and White, 1986; White and McKenzie, 1989; Watson and McKenzie, 1991; Griffiths and Campbell, 1991). Another contribution to transient uplift is generated if the lithosphere is reheated and thinned as it passes over the plume (Detrick and Crough, 1978; Crough, 1978). Conductive heating and cooling of the lithosphere occurs too slowly to explain significant vertical motions over the short

time periods of LIP emplacement. More rapid thinning of the lithosphere might occur if the convecting mantle can remove the base of the lithosphere by mechanical erosion, secondary convection or gravitational instability (Spohn and Schubert, 1982; Liu and Chase, 1989; Sleep, 1994; Şengör, 2001; Elkins-Tanton, 2005). Uplift generated by all of these mechanisms should dissipate after the plume has gone.

Permanent surface uplift arises when magma extruded at the surface, or injected into the crust or uppermost mantle ('underplating' of the crust), causes isostatically compensated uplift, which persists after the plume has gone (Cox, 1989; White and McKenzie, 1989). A related component of permanent uplift arises because extraction of basaltic melt reduces the density of the mantle residue or restite (White and McKenzie, 1989). Melt extraction buoyancy produced by restite may account for up to about half of the surface uplift in the modern Hawaiian swell (Morgan et al., 1995). Permanent uplift is more difficult to interpret than transient uplift because models for melting and melt transport are also required in order to infer mantle temperature and convective structure.

Recently, the long-accepted model of flood basalt volcanism requiring plume head melting with associated rifting and mantle decompression (e.g. Richards et al., 1989; White and McKenzie, 1989; Campbell and Griffiths, 1990; White and McKenzie, 1995; Ernst and Buchan, 2003) has been challenged (Anderson, 1994, 2000, 2001; Sheth, 1999, 2005). If the plume head model is correct, then the predicted transient surface uplift and subsidence should generate an erosional or depositional signature in terrestrial and marine sedimentary basins across and adjacent to the main uplifted region. Two main problems complicate interpretation of the sedimentary record in terms of transient dynamic surface uplift. First, recognition of dynamically supported uplift and subsidence depends on being able to separate out vertical motions generated by past or ongoing extension or shortening of the lithosphere. In practice, this separation can only be achieved when both the pre-existing topography and the long-term subsidence history can also be interpreted from the geological record. Second, surface uplift often leads to erosion. Even when the magnitude of erosion can be measured accurately, isostatic adjustments of surface level that result from erosion mean that it is often difficult to retrieve accurate estimates of the original surface uplift unless *a priori* constraints on timing of uplift and erodibility of the material are available (Molnar and England, 1990a). In the context of the mantle plume debate, it should also be noted that observations of transient surface uplift do not directly constrain the depth of origin of the upwelling mantle.

In this paper, we initially summarise the main models that have been proposed for LIP formation and discuss how these models might be constrained by geological observations. We then review the evidence for the nature and extent of uplift associated with four continental LIPs and one continental hotspot (Emeishan Traps, Siberian Traps, Deccan Traps, North Atlantic Igneous Province, and Yellowstone). Each province is presented as a case study, focussing on evidence for transient uplift and the relationships between uplift, rifting and magmatism. We then compare and contrast the observations from the five provinces. Because the tectonic setting of each LIP is unique, the effect of surface uplift, rifting and magmatism on the geological record is also unique, so that comparisons between provinces need to be made with care. Bearing this potential difficulty in mind, we discuss the implications of the observations for plume and non-plume models of mantle convection.

2. Mechanisms of LIP formation and predicted consequences for uplift

The defining characteristic of LIP formation is the geologically rapid eruption (within a few million years) of unusually large volumes of magma, mainly silica-saturated basalt or tholeiite. It is usually accepted that rapid and voluminous melt generation requires decompressional melting. (We do not consider the alternative case in which energy to cause rapid voluminous melting is supplied externally by a meteorite impact, since none of our observations from the provinces considered here suggest this scenario). Decompression is an efficient mechanism for generating large amounts of melt because the adiabatic temperature gradient (about 0.6 °C/km; McKenzie and Bickle, 1988) is much steeper than the gradient of the solidus both for anhydrous mantle peridotite (about 4–5 °C/km at lithospheric depths) and for more enriched mantle compositions (Hirschmann and Stolper, 1996). Upwelling of mantle to cause decompressional melting can be active, driven by buoyancy forces that set up a convective circulation, or passive, in response to thinning of the lithosphere. In this section, we first discuss two families of models for active upwelling. In one family, convection is controlled by lateral density variations related to heating within or at the base of the mantle (often described as mantle plume models), whereas in the other, convection is controlled mainly by lateral density variations related to cooling of the plates (often described as top-down convection models). We also

discuss models for how the lithosphere deflects in response to mantle convection. We then consider mechanisms for thinning the lithosphere, which include both rifting and removal of the base lower part of the mantle lithosphere by gravitational instability in response to mantle convection.

All of the decompression melting scenarios listed above could operate simultaneously. For example, where a plume supplies hot mantle beneath the lithosphere, enhanced melting would occur in regions of coeval or recent rifting, and melting could be further enhanced by small-scale convection beneath these rift zones. It is useful to view the current mantle plume debate as a chance to weigh up the relative roles of all these processes in individual provinces. Melt production may also be enhanced in all of these models if the peridotite source is particularly fertile (e.g., contains eclogite or pyroxenite) or volatile-rich. However, active or passive upwelling is always required to transport the enriched source material into the melting region.

2.1. Mantle plumes

In mantle plume models, upwelling is initiated by lateral buoyancy variations deep in the mantle. It is usually accepted that the positive buoyancy results mainly from higher heat content, although compositional buoyancy may play a role. Thermal buoyancy may be supplied by both internal and basal heating. A component of basal heating is required to generate concentrated upwelling in a plume conduit rather than diffuse upwelling over a broad region, although it need not be a large component (Bunge et al., 1997). The importance of basal heating implies that mantle plumes must rise from a thermal boundary layer, and the most likely candidates are generally thought to lie just above either the core-mantle boundary or the 670-km discontinuity. Recent more earth-like numerical experiments that account for the depth dependence of thermal expansivity and realistic plate motions suggest that narrow concentrated plumes need not be directly related to the core-mantle boundary or the 670-km discontinuity and they can sometimes rise from the edges of hot bodies ponded in the mid mantle (Davies and Bunge, 2006). Unfortunately, observations of surface uplift cannot distinguish these models for plume initiation because deflection of the surface of a fluid layer is mainly a response to motion of the fluid close to the surface (Parsons and Daly, 1983). Therefore observations of uplift at Earth's surface can constrain models for impact of a plume head beneath the lithosphere, while seismic constraints on the topography of the core-mantle

boundary and 670 km discontinuity would be required to constrain models for plume initiation.

When the buoyant peridotite rises to the base of the plates, it may decompress sufficiently to undergo extensive melting, typically forming large volumes of tholeiitic basalt magma. One explanation of the formation of LIPs is that they represent an anomalous transient period of high plume flux, perhaps associated with an initiating, or 'start-up' plume. The predicted shape and rise time of start-up plumes are strongly dependent on assumptions about mantle viscosity structure, rheology and the relative importance of internal and basal heating. In a Newtonian, isoviscous fluid with all buoyancy supplied from below, starting plumes form roughly spherical diapirs (Richards et al., 1989; Campbell and Griffiths, 1990; Griffiths and Campbell, 1991). When this model is applied to explain LIPs, the diapir (or plume head) needs to be initially about 1000 km in diameter and, on impact with the base of the lithosphere, the head is predicted to spread laterally to form a structure some 2000 km in diameter. However, the viscosity in the mantle probably decreases by several orders of magnitude from bottom to top (Forte and Mitrovica, 2001). In this case, diapiric plume heads are predicted to narrow and rise more rapidly towards the top of the mantle (Farnetani and Richards, 1994). If the mantle rheology is strongly non-linear, then start-up plume heads are predicted to be only a few hundred km in diameter, similar to the diameter of the trailing plume conduits (Larsen et al., 1999). If the asthenosphere forms a particularly low viscosity channel, then convective flow should be strongly concentrated in this layer. This argument has lead to development of a group of plume head models that ignore the dynamics of buoyant material rising through the mantle and concentrate on lateral flow within the asthenosphere (Ribe and Christensen, 1994; Sleep, 1996, 1997).

Two of the main observations of interest in this study are the timing and magnitude of surface uplift and the spatial and temporal relationship between uplift and magmatism. Although start-up plume models generally predict that uplift should precede magmatism, more detailed prediction of the responses listed depends on the choice of model as well as the viscosity structure and rheology. At one end of the spectrum, the diapiric start-up plume model of Griffiths and Campbell (1991) predicts that uplift may begin about 20 m.y. and peak about 5 m.y. before onset of igneous activity. On the other hand, plume head models dominated by lateral asthenosphere flow with non-linear rheology allow onset and peak of uplift to be less than 1 m.y. before onset of igneous activity (Larsen et al., 1999). The

maximum amplitude of uplift is predicted to be about 0.5–1 km for diapiric models (Campbell and Griffiths, 1990) or higher if the temperature anomaly is hot enough to generate significant melt below unstretched lithosphere (Farnetani and Richards, 1994). Lateral spreading plume head models can explain uplift of up to several kilometres (Sleep, 1997). These figures can be compared with estimates of modern dynamic support of about 2 km at Iceland and 1.2 km at Hawaii (Sleep, 1990; Jones et al., 2002). The spatial relationship between uplift and igneous activity depends on the relative importance of upwelling and lateral spreading of plume material, and on the thickness of the lithosphere. If significant upwelling occurs (diapir models) then igneous activity should occur across the uplifted region. If the plume head is injected laterally then all decompressional melting should occur near the plume conduit, and large regions away from the conduit can experience major uplift but little igneous activity. However, both of these scenarios will be modified by lithospheric thickness. Overall there are no detailed constraints on timing and amplitude of uplift from the plume head models, mainly because the viscosity structure of the mantle is not sufficiently well known. It is therefore better to constrain the models using observations rather than to judge the observations using the models.

2.2. 'Top-down' convection models

In top-down convection models, the lateral thermal gradients required for convection are generated by lateral differences in lithospheric thermal insulation and/ or by topography on the base of the lithosphere. Convection is confined in the upper mantle in many models, although it penetrates the lower mantle in some variants (Korenaga, 2004). Juxtaposition of many continent-based LIPs with the margins of cratons led Anderson et al. (1992) and King and Anderson (1995) to propose that the thermal contrast beneath cratonic lithosphere and the adjacent thinner lithosphere initiates a convection cell. As the mantle flows out from under the craton in the upper limb of this convection cell, it may upwell, decompress and melt beneath the thinner lithosphere. This style of convection was termed a 'hotcell' by Anderson et al. (1992). Guillou and Jaupart (1995) have proposed that thermal insulation beneath continents may actually establish plume-like convection systems. In another top-down scenario known as edge-driven convection, a convective cell is set up adjacent to a sharp step in lithospheric thickness. The sharp step could be the edge of a craton (King and Anderson,

1995), the boundary between very old oceanic lithosphere and thinner continental lithosphere (King and Ritsema, 2000) or the margin of a narrow rift zone (Mutter et al., 1988). Edge-driven convection could form a secondary circulation within a hotcell (King and Anderson, 1998). Mutter et al. (1988) proposed that active upwelling rates might be further enhanced by the increase in buoyancy of residual mantle upon melting, though it is also possible that the concomitant increase in viscosity could suppress secondary convection. All of the studies mentioned above suggest that generation of volcanic passive margins can be explained by edge- and residual buoyancy-driven convection alone and need not be linked to upwelling of unusually hot mantle from great depth. However, edge-driven convection could also occur as secondary convection within a plume head, where it would be even more effective in enhancing melt production because of the higher temperature and lower viscosity (Keen and Boutilier, 2000). Observations of surface uplift provide a clear test of whether convection is related to lithospheric architecture. In the hotcell model, cratons overlie hot upwelling mantle and should be uplifted, whereas the adjacent thinner lithosphere should overlie the down-welling limb and should remain stable or subside. In the edge-driven convection model, uplift should occur in a band parallel to the lithospheric step.

2.3. Response of the lithosphere to convection

The lithosphere is generally thought to deflect passively in response to underlying thermal and convective structure to give long-wavelength (many hundred to a few thousand km diameter) domal surface uplift. The strength of the lithosphere means that it potentially filters out short-wavelength features, such as the steep flow fronts predicted by some plume head models based on laterally spreading gravity currents, or small-scale edge-driven convection cells. These views come from observations of modern oceanic hotspot swells, described in the introduction. However, Burov and Guillou-Frottier (2005) argue that a rheologically layered lithosphere can lead to a much more complex surface response. They predict that simple, long-wavelength doming should occur only in cases where the lithosphere contains no weak internal layers, and they suggest that this condition is met only in oceanic and old, cold and thick continental lithosphere. In situations where the continental lower crust is weak and there is good coupling between lithosphere and asthenosphere, they show that either surface uplift or subsidence can occur over a range of amplitudes and

wavelengths in response to a mantle plume head. However, the continental rheology used by Burov and Guillou-Frottier (2005) could be a special case. There is evidence that in many continental regions the lower crust is strong and dry and the underlying asthenosphere is weak (Morgan et al., 1995; Maggi et al., 2000) and in these cases the surface response to a mantle plume should be the same as in the oceanic case. The Burov and Guillou-Frottier (2005) surface uplift model therefore needs to be tested using observations from LIPs emplaced in a range of continental tectonic settings. Data from the Emeishan and North Atlantic Provinces are useful in this regard. These data provide no obvious evidence for complex spatial patterns of surface uplift.

2.4. Lithospheric thinning

The major element composition of flood basalts shows they are usually produced beneath thin lithosphere (Jaques and Green, 1980). More recently, rare earth element modelling has shown that the top of the melting zone for many major flood basalt provinces lay well within the spinel stability field, at a depth of 50–70 km (White and McKenzie, 1995). Lithospheric thinning to explain these observations might occur by gravitational instability and/or by rifting.

If lithospheric thinning occurs only by rifting, the amount of rifting required to account for the observed melt production rates and compositions depends on whether mantle upwelling is passive or active. For active upwelling, stretching of the lithosphere by a factor of less than 2 is required to account for melting rates appropriate for the Deccan, North Atlantic and Siberia (White and McKenzie, 1995). Rifting can be coeval with magmatism or it can precede magmatism by a time period of less than one lithospheric thermal time constant (40–60 m.y.) to leave lithospheric 'thin spots' (Thompson and Gibson, 1991). Greater amounts of stretching are required if upwelling is passive. Melt production during rifting can be increased by increasing the magnitude of stretching or by decreasing the duration of stretching, as well as by increasing the mantle potential temperature (Bown and White, 1995).

The lithosphere comprises an upper mechanical boundary layer, in which heat is entirely transported by conduction, and a lower thermal boundary layer, which is subject to episodic convective instabilities that maintain equilibrium plate thickness (White, 1999). The base of the mechanical boundary layer lies about 100 km deep beneath mature oceanic lithosphere and greater than 150 km deep beneath cratons (White,

1999). If hot mantle is emplaced beneath the lithosphere, gravitational instabilities can remove the lithospheric thermal boundary layer relatively easily (Davies, 1994). However, mantle convection alone cannot easily erode the base of the mechanical boundary layer because heat is mainly transported in to it by conduction, a slow process. In this case, rifting is also required to explain rapid melting much shallower than about 100 km for equilibrium lithosphere. Alternatively, if sufficient heat can be introduced into the mechanical boundary layer by intrusion of dykes, the entire mantle lithosphere can potentially be weakened and removed by gravitational instability, allowing shallow melting without any need for rifting (Tanton and Hager, 2000; Elkins-Tanton, 2005).

The processes of thinning the lithosphere by stretching and by gravitational instability are not identical, but are similar enough to generate transient surface uplift histories that are probably indistinguishable in practice. A better way to constrain the roles of rifting and gravitational thinning is therefore to measure the rifting history from subsidence analysis of sedimentary successions, observations of fault movements and seismic profiling of the entire crust. If rifting can account for the thinning that is required to explain the observed melt volumes and compositions, then gravitational instabilities need not be invoked. However, this procedure will be difficult where seismic imaging is sparse or an incomplete sedimentary record of rifting is preserved.

3. Emeishan Traps (~260 Ma) (Yigang Xu)

The Late Permian Emeishan basalts are erosional remnants of the voluminous mafic volcanic successions occurring in western margin of the Yangtze Craton, southwest China. They are exposed over an area of 250,000 km^2 (Zhang et al., 1988; Xu et al., 2001) bounded by the Longmenshan thrust fault in the northwest and the Ailaoshan–Red River strike-slip fault in the southwest (Fig. 1a). However, some basalts and mafic complexes exposed in the Simao Basin, northern Vietnam (west of the Ailaoshan–Red River Fault), and in Qiangtang terrain, Lingjiang–Yanyuan belt and Songpan active fold belt (northwest of the Longmenshan Fault) may be parts of the Emeishan LIP (Chung et al., 1998; Xiao et al., 2003; Hanski et al., 2004). The Emeishan volcanic succession comprises predominantly basaltic flows and pyroclastic deposits, with minor amounts of picrites and basaltic andesites, with a total thickness ranging from several hundred metres up to 5 km (Chung et al., 1998; Xu et al., 2001).
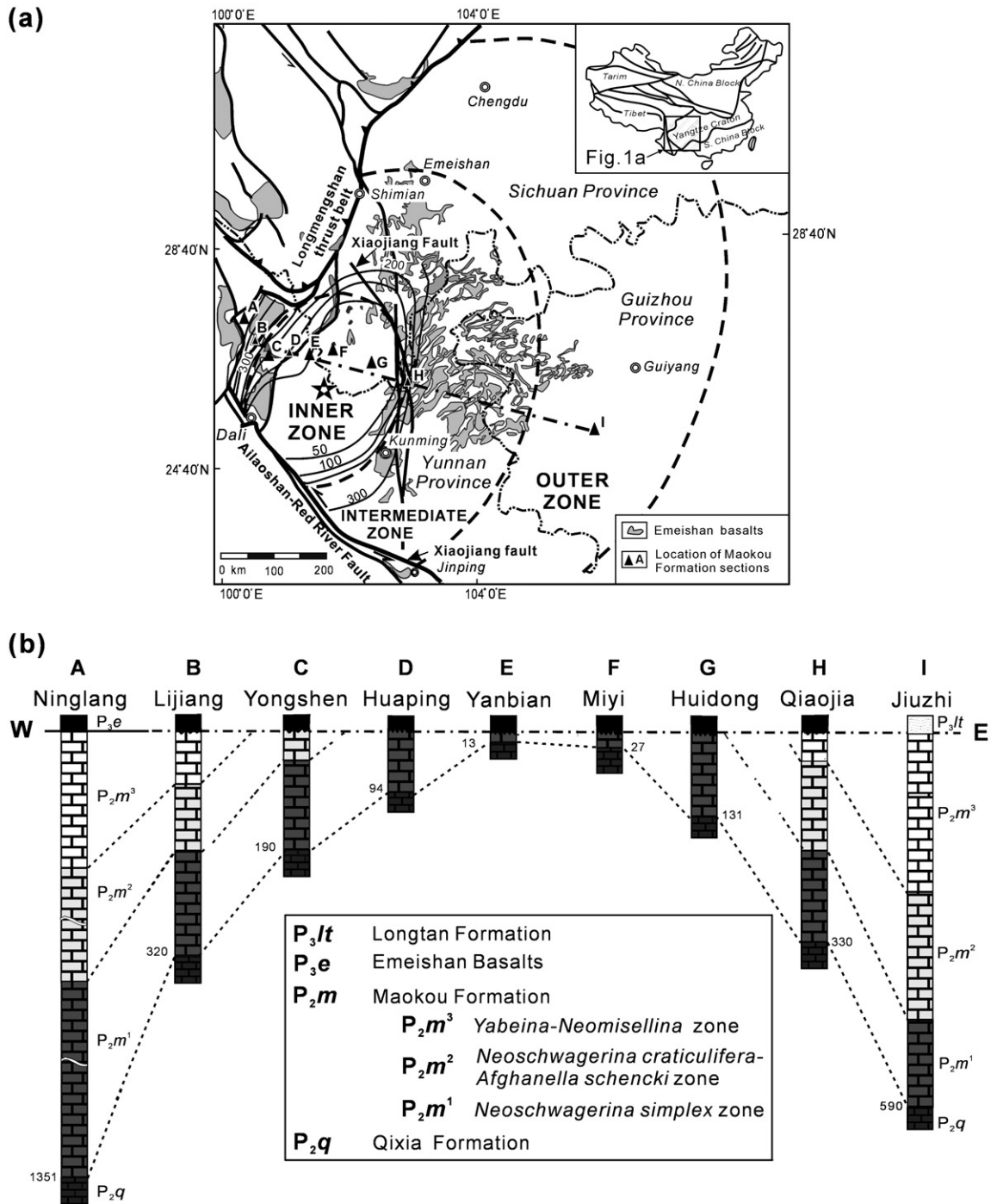
(a)

(b)

Fig. 1. (a). Map showing geology of the Emeishan large igneous province and the isopachs of the Maokou Formation. Numbers on isopachs indicate the thickness in metres. Dashed lines separate the inner, intermediate and the outer zones, which are defined in terms of erosion extent of the Maokou Formation. (b). Biostratigraphic correlation of the Maokou Formation in the Emeishan large igneous province along the west-east oriented profile shown in (a). (Stratigraphic columns A to I correspond with locations along the profile.) Modified after He et al. (2003).

The Emeishan basalts unconformably overlie an upper Middle Permian carbonate, the Maokou Formation, and are in turn covered by the uppermost Permian Xuanwei and Longtan Formations (equivalent to the Wujiaping Formation) in the east, and the Late Triassic sedimentary rocks in the central part, of the Emeishan

LIP. It is now clear that the contact between the Triassic sedimentary rocks and the Emeishan basalts is an erosional unconformity, which resulted from prolonged uplift of the central Emeishan LIP and concomitant erosion of Emeishan basalts (He et al., 2006). The stratigraphic relationship therefore suggests that the Emeishan basalts were erupted prior to the Permo–Triassic boundary, most likely occurring at the Middle-Upper Permian boundary (corresponding to the Capitanian/Wuchiapingian stage: 260 Ma; Gradstein et al., 2004). Consequently, the eruption age of the Emeishan basalts is inferred to be ~260 Ma (Courtillot et al., 1999; Xu et al., 2004). This age is confirmed by recent U–Pb analyses on zircons from the mafic and alkaline intrusions (Zhou et al., 2002; Xu et al., unpublished data).

3.1. Evidence for pre-volcanic uplift

The sedimentation in SW China prior to the Emeishan flood volcanism is characterized by a carbonate platform setting (Wang et al., 1994; Feng et al., 1997). This carbonate platform, covering an area much larger than the Emeishan LIP, comprises the Liangshan, Qixia and Maokou Formations. Based on the petrologic characteristics of the limestone and associated fossil assemblages, the seawater in south China in the Permian period is inferred to have been shallow and clean, and by implication the crust was stable at that time.

The main constituent of the carbonate platform, the widespread Maokou Formation, immediately underlies the Emeishan basalts. It mainly consists of bedded to massive limestones, and has a thickness ranging from 250 to 600 m. An abundant and rapidly evolved fossil assemblage permits division of the Maokou Formation into three biostratigraphic units, from bottom to top, *Neoschwagerina simplex* zone, *Neoschwagerina craticulifera–Afghanella schencki* zone and *Yabeina–Neomisellina* zone (Fig. 1b). These biostratigraphic units are well correlated throughout south China (ECS, 2000), and thereby permit a regional-scale comparison (Fig. 1).

Integration of the data from 67 sections allows the construction of isopachs within the Maokou Formation. These isopachs delineate a subcircular plan (Fig. 1a). The thickness varies from <100 m in the inner zone, through 200–450 m in the intermediate zone, to ~600 m in the outer zone (He et al., 2003). The inner zone encloses west Yunnan and south Sichuan, and is about 400 km in diameter (Fig. 1a). A cross section across the region (Fig. 1b) also clearly shows the thinning of the Maokou Formation in the inner region. For instance, while all three biostratigraphic units of the Maokou

Formation are present in the sections at the two ends of the profile (especially in Guizhou province), only the lowermost unit (i.e., the *Neoschwagerina simplex* zone) is present in the sections in the central part of the profile (Fig. 1b).

The regional variations in the thickness and distribution of the Maokou Formation could be due to differential erosion, or absence of a suitable depositional basin due to lack of basement subsidence. Although different in detail, both scenarios require crustal domal uplift in the middle-late Permian.

The contact between the Maokou Formation and the Emeishan basalts in the inner and intermediate zones is irregular, with considerable topographic relief. The majority of Emeishan basalts were erupted subaerially (Chung et al., 1998), and were probably emplaced over a karstic surface of the Maokou Formation. The relief of the contact is usually several metres to 50 m high (He et al., 2003). Limestone enclaves or blocks are commonly found in the lower volcanic succession in the southern part of the Emeishan LIP. The enclaves may originally have been gravels, boulders or blocks on erosion surface that were then entrained by lavas during emplacement. Karst morphology developed at the top of the Maokou limestone, and is well preserved at Lunan (approximately 75 km SE of Kunming). The development of karst morphology requires exposure of the Maokou Formation under subaerial conditions. This could be taken as evidence for crustal uplift prior to the Emeishan volcanism.

Other evidence in support of the idea that the contact between the Maokou Formation and Emeishan basalts is an erosion surface or a depositional hiatus includes: (a) in some localities in the inner and intermediate zones, there are relict gravels, boulders and basal conglomerates along the contact; and (b) palaeoweathering crust and palaeosols occurring along the contact between the Maokou Formation and the Emeishan basalts in the outer zone. The palaeoweathering zone contains pyrite-bearing clay rocks, manganese and thin layers of coal and siliceous rock.

It is important to note that the unconformity is regional and restricted to the Emeishan LIP, and is not observed in the southern Yangtze and South China Blocks. The thinned Maokou Formation capped by an unconformity suggests that the development of the uncomformity was induced by crustal uplift, which was also responsible for the stratigraphic thinning.

The Middle Permian is characterized by the deposition of a vast carbonate platform (Fig. 2a). This platform was subjected to subaerial erosion to varying degrees in the late Middle Permian, leading to the appearance of an

elliptical basement core (known as the Chuandian 'old land') in the centre of the Emeishan LIP (Fig. 2b). Late Permian palaeogeography is defined by deposition on and offlapping from this "circular" region. For example the distribution of upper Permian post-basalt terrestrial clastic sedimentary rocks (Xuanwei Formation) is largely confined to the intermediate zone surrounding the Chuandian old land, and the shallow marine limestones (Longtan Formation) tend to have been deposited in the outer zone (Fig. 2b). The transition from terrestrial to shallow marine clastic sedimentation and the circular sedimentary pattern are expected given the crustal doming in the Emeishan LIP.

The distribution of the Emeishan basalts appears to be correlated with the spatial variation in thickness of the Maokou Formation. Most of the remaining outcrops of the Emeishan basalts occur within the intermediate zone, whereas there are few, localised outcrops of basalt in the inner zone. This distribution pattern can be understood if the inner zone corresponds to the uplift area where originally emplaced basalts were largely removed due to enhanced erosion. Recent geochemical analyses of clastic rocks of the Xuanwei Formation, which occurs surrounding the inner zone (Fig. 2b), show that the lowermost rocks have a geochemical affinity to the Emeishan felsic volcanic rocks, whereas the overlying sediments are compositionally more akin to mafic components of the Emeishan traps. This is the reverse of volcanic sequence of the Emeishan LIP where the felsic extrusives sit above predominantly mafic rocks. We thus suggest that the Xuanwei Formation comprises water-transported sedimentary rocks resulting from erosion of the volcanic rocks in the centre of the Emeishan LIP (He et al., 2006).

3.2. Timing, scale and extent of the uplift

The stratigraphic thinning of the Maokou Formation could be related to differential erosion or lack of subsidence and accumulation. Although both cases require crustal uplift, they imply different timing. If the stratigraphic thinning is related to sedimentation over an already uplifted region, uplift might have taken place after the formation of lowermost unit of the Maokou Formation, given the presence of the *Neoschwagerina simplex* zone in the centre of the uplift area. In this case, the crust was uplifted above sea-level after the early Middle Permian; consequently, the two upper units were not accumulated in the uplifted area. However, several lines of evidence suggest that all three units of the Maokou Formation had been accumulated in South China and that formation thinning may be related to subsequent erosion. For example, conglomerates on the erosional surface, in alluvial fans and limestone lenses in the lower lava successions in the inner and intermediate zones contain fossils that are identical to those found in the uppermost Maokou Formation (He et al., 2003). Therefore, the domal uplift likely started after, or was coeval with, the deposition of the uppermost unit of the Maokou Formation. The duration of pre-eruptive uplift has been estimated to be 1–2.5 m.y. by using the eroded thickness of the Maokou Formation and erosion rates under tropical climate conditions (He et al., 2003).
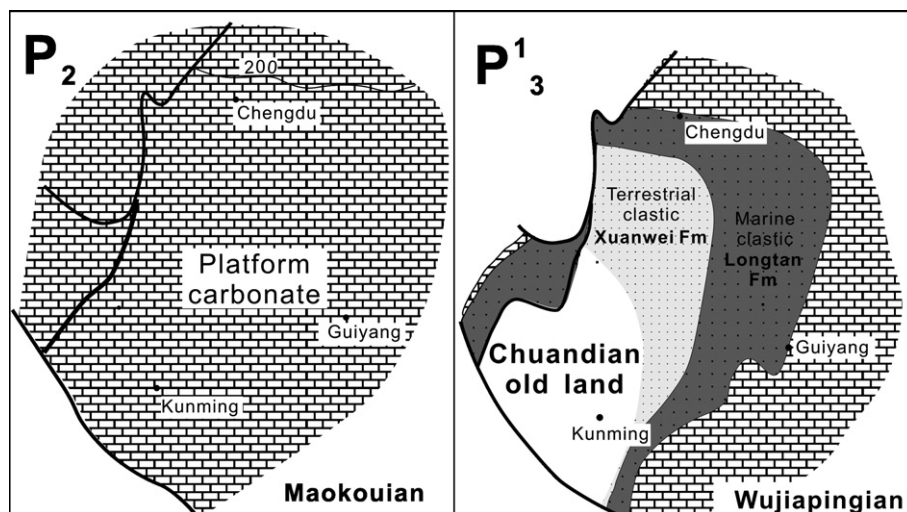

Fig. 2. Comparison of palaeogeography before and after the Emeishan volcanism. (a) A stable, homogeneous carbonate platform in the Maokou stage (P_2); (b) palaeogeography in the Wujiapingian (P_3^1) showing clastic rocks surrounding the Chuandian old land. Modified after Xu et al. (2004).

The persistence of the Chuandian old land until the middle Triassic suggests a prolonged uplift (>45 Ma) of the inner zone in the Emeishan LIP. This uplift may be composed of two phases separated by rapid subsidence. Evidence for this includes: (a) although the majority of Emeishan basalts were subaerially erupted, small portions of submarine facies occur in the margin of the Emeishan LIP (He et al., 2006). (b) The uplift probably ended in the beginning of the Late Permian (~258 Ma) because a new transgression and depositional onlap started at that time (Xu et al., 2004). These observations suggest a rapid subsidence phase following the pre-volcanic uplift.

According to the spatial distribution of the thinned Maokou Formation and of the unconformity between the Emeishan basalts and the Maokou Formation, the uplifted area is inferred to cover nearly entirely the western part of the Yangtze Craton. It corresponds to an area 800 km in radius (Fig. 1a). The magnitude of

dynamic uplift has been estimated from the erosional features in the overlying sedimentary sequence (He et al., 2003). A lower bound of 50–100 m of uplift is obtained from the observed exhumation of 500 m by isostatic balancing. An estimate of >1000 m of uplift has been inferred by He et al. (2003) on the basis of the geometry of the alluvial fan in the northeastern flank of the domal structure.

4. Siberian Traps (~251 Ma) (Andy Saunders)

The Siberian Traps represent the remnants of the largest Phanerozoic continental flood basalt province, with an estimated original area of 4×10^6 km^2 and an original combined volume of extrusive and shallow intrusive rocks at least 2×10^6 km^3 (Milanovskiy, 1976) but probably significantly more (Fedorenko et al., 1996). Eruption was coeval with the Permo–Triassic boundary at 251 Ma (using the timescale of Gradstein et al., 2004).
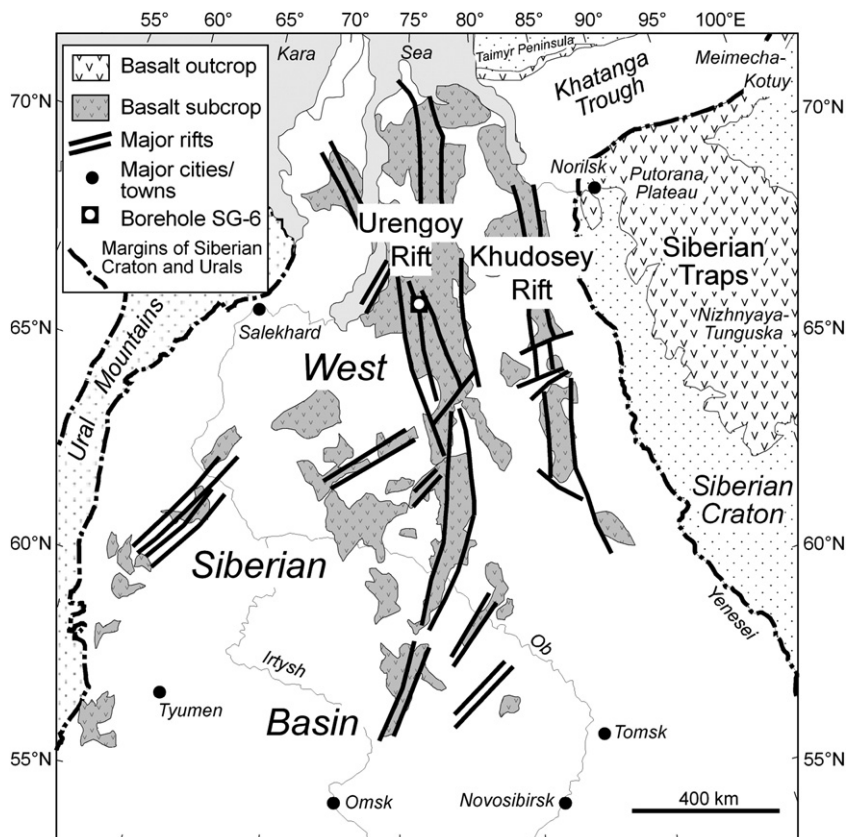

Fig. 3. Map of the West Siberian Basin and adjacent terrain showing the location of the outcropping Siberian Traps on the Siberian Craton and Taimyr Peninsula, and the estimated extent of the basalts beneath the West Siberian Basin. The precise area and age of the basalts within the West Siberian Basin are unknown; many are buried several kilometres beneath Mesozoic and Cenozoic sedimentary rocks. The western margin of the Siberian Craton is approximately followed by the Yenesei River. (After Surkov, 2002; Reichow et al., 2005; Saunders et al., 2005).

Isotopic dating reveals that the bulk of the lavas and intrusive rocks at Noril'sk, northern Siberia (Fig. 3), were erupted in a short time period (less than 1 m.y.), but the duration of the province as a whole is unknown; it may be a short as 600 k.y. (Campbell et al., 1992), but could be much longer. Isotopic dates from widespread localities, including Meimecha–Kotuy, the West Siberian Basin and Putorana (Fig. 3) all indicate magmatic activity around 250 Ma, so it is likely that the bulk of the province was erupted synchronously (see reviews in Reichow et al., 2002; Kamo et al., 2003). A substantial portion of the Siberian LIP is, unfortunately, buried beneath the West Siberian Basin and the Khatanga Trough. The maximum observed thickness (~3500 m) of lavas occurs at Noril'sk (e.g. Wooden et al., 1993) located on the NW margin on the Siberian Craton, but the thickness beneath the Khatanga Trough may be substantial, and several kilometres of basalt are known to exist in deep graben structures beneath the West Siberian Basin (Westphal et al., 1998). The rift structures beneath these basins define a crude 'triple junction' which has been invoked as the main focus of activity of the Siberian Traps.

The involvement of a mantle plume in the formation of the Traps has been questioned on the basis of field data. Czamanske et al. (1998) have argued that the Permian and Triassic sedimentary facies on the Siberian Craton in the areas of Noril'sk, Putorana and Nizhnyaya–Tungsuka show no evidence of uplift, transient or otherwise, as predicted by emplacement of a mantle plume beneath those regions. Indeed, there may even be indication of subsidence, because brackish and possibly marine fossil fauna are found in intertrappean sediments. However, all of these successions lie on the Siberian Craton, a region of very thick lithosphere that has remained tectonically stable since at least the Palaeozoic. Furthermore, it is not clear where the putative plume ascended; beneath the craton or beneath the basins to the north and west.

The West Siberian Basin has acted as a major depositional centre throughout most of the Mesozoic and Cenozoic (Peterson and Clarke, 1991). Deep N–S grabens and half-grabens show up on seismic profiles of the basement surface (Fig. 3, and Surkov, 2002). The rifting event(s) that formed these grabens was active at least during the Triassic and possibly into the Jurassic, but it is not clear when rifting began (Saunders et al., 2005). Many of the rifts are floored by thick sequences of basalt, but basalt also occurs on the rift shoulders (Fig. 3), so it would appear that at least some of the volcanism either pre-dates, or was synchronous with, the rifting events. Reichow et al. (2002, 2005) have confirmed that at least some of the basalts are con-

temporaneous with, and compositionally similar to, the main Traps exposed to the east. Although the basement surface now lies several kilometres below sea-level, this was not the case during the late Palaeozoic (Peterson and Clarke, 1991). Early sedimentary rift fill is characterized by Triassic continental facies which inter-finger with marine facies in the northern part of the basin. Structural highs in the Palaeozoic basement surface were emergent until the Jurassic. Jurassic sedimentary rocks lie with major unconformity on the Palaeozoic basement on the rift shoulders and on regional horsts, indicating major marine incursions at that time. There are surprisingly few Permian sequences preserved, suggesting that the region was undergoing erosion, or non-deposition, at that time. Whether this was due to uplift associated with the emplacement of a mantle plume or a regional orogenic process is unclear.

The basalts from Noril'sk show a progressive shallowing of the average depth of melting through the 3500 m thick sequence. The early lavas (e.g., the Gudchikhinsky Suite) have Sm/Yb ratios consistent with melt generation beneath moderate-thickness lithosphere (~100 km, similar to that beneath Hawaii), but the Sm/Yb ratios decreased markedly in the later voluminous Upper Sequence (e.g., Fedorenko et al., 1996; Sharma, 1997). These data indicate very shallow depths of melt segregation, entirely at odds with melt generation beneath the thick Siberian Craton or indeed beneath any typical continental lithosphere. The present-day thermal thickness of the craton is of the order of 300 km (Artemieva and Mooney, 2001), consistent with the seismological evidence (Zhang and Tanimoto, 1993) and, whilst we are uncertain about the thickness of the craton during the Permian, there is no reason to believe that it was significantly thinner than at the present-day. Generation of tholeiites beneath such thick lithosphere, whilst simultaneously producing the observed low Sm/Yb ratios, would require very high mantle temperatures with attendant strong uplift. Rather, the data indicate melt generation beneath highly thinned lithosphere, beneath the lithosphere of the West Siberian Basin and adjacent basins.

Such attenuation may have been achieved by prior or contemporaneous rifting and indeed there is clear evidence of Permo–Triassic rifting in the West Siberian Basin, forming the large Urengoy and Khudosey rifts (e.g., Nikishin et al., 2002; Saunders et al., 2005; Vyssotski et al., 2006; Fig. 3). The amount of extension (β factor) was estimated by Saunders et al. (2005) to be between 1.2.and 1.6 which, because of magmatic additions, must be considered a lower bound. If the amount of synmagmatic strain in the West Siberian Basin was of the order of 2 to 3, and was rapid, then it is theoretically

possible to generate 1 to 2 km of melt from mantle with a potential temperature of 1400 °C (e.g., Bown and White, 1995). However, it should be emphasized that a significant part of the rifting was Triassic and post-Triassic in age, because sediments as young as Jurassic are involved in growth faults at the graben margins. There appears therefore to be a contradiction in the amount of extension predicted by the amount and composition of the basalts, and the amount of extension estimated from the crustal structure.

5. Deccan Traps (~65 Ma) (Mike Widdowson)

The Upper Cretaceous to Lower Paleocene Deccan Traps currently extend over an area of ~500,000 km², and are estimated to have had an original erupted volume of $0.75–1.5 \times 10^6$ km³ (Fig. 4). The Deccan is perhaps the most widely known and discussed of all the continental flood basalt provinces, due largely to its eruption being contemporaneous with the Cretaceous–Tertiary boundary (KTB) (Baksi and Ferrar, 1991; Basu et al., 1993; Baksi, 1994; Widdowson et al., 2000; Fig. 5). Much of the main Deccan province was erupted between 66–65 Ma over a period of only 0.5–1 m.y. (Duncan and Pyle, 1988; Courtillot et al., 1988), mostly during chron 29r (Courtillot et al., 1986; Gallet et al., 1989; Hofmann et al., 2000). Its postulated origin from melting of a plume head has recently been challenged (e.g., Sheth and Chandrashekharam, 1997; Sheth 1999, 2005).

5.1. The timing of rifting and Deccan volcanism

The relative timing of rifting, separation of continental fragments, and volcanism is crucial to both the plume and the non-plume models. One variant of the plume model is that rifting above an incubating plume
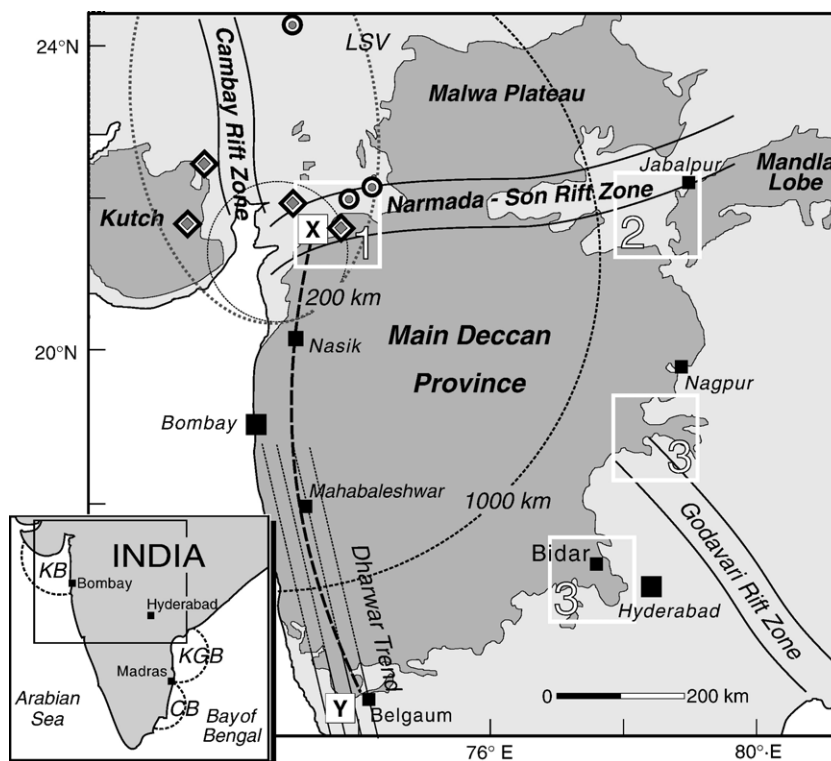
Fig. 4. Map of the Deccan flood basalt province showing main structural components. Shaded areas represent the current areas of basalt outcrop. Cross section (Fig. 6) line X–Y follows the Western Ghats escarpment where the lava succession is best exposed. Oval region (dotted) marks the limit of a low seismic velocity zone (LSV) beneath the Indian continental crust; Kennett and Widiyantoro (1999) argue this LSV marks the region where the plume head conduit penetrated beneath the Indian continental crust. A 200 km diameter circle marks the region of maximum predicted uplift above a putative plume sited beneath the junction of the Narmada and Cambay rift zones at c. 70–68 Ma. A 1000 km diameter circle marks the limit of uplift generated by the same plume. The locus of dynamic plume-related uplift migrated southward as a consequence of the northward drift of greater India. Numbers 1–3 (square boxes) indicate the localities of key onshore sedimentary successions. Inset map shows location of major offshore depocentres; Kutch Basin (KB); Krishna–Godavari Basin (KGB); Cauvery Basin (CB). Bulls-eye circles show position of alkaline complexes, and diamonds indicate location of primary picritic basalts.
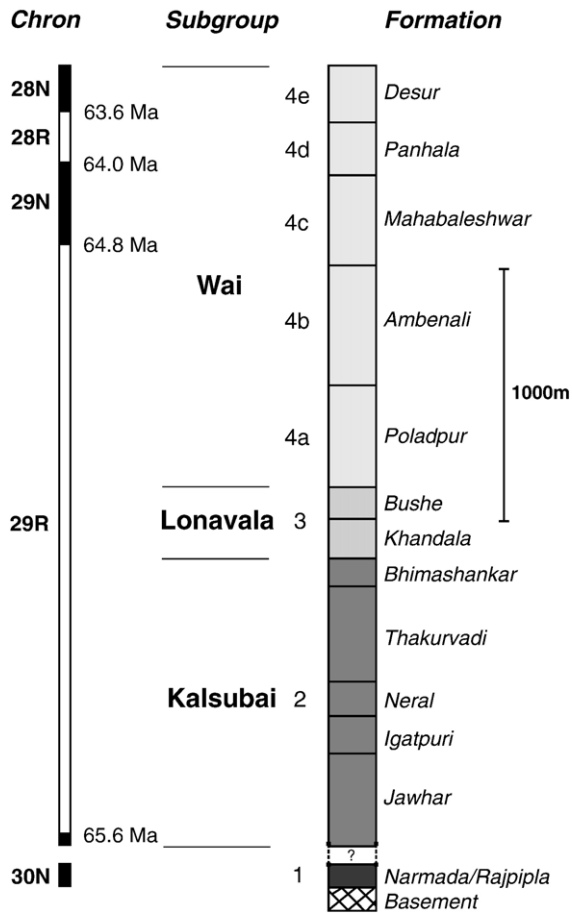
Fig. 5. Composite chemostratigraphy and magnetostratigraphy of the main Deccan province. Individual formational units are shown to approximate thickness. Age data are provided for magnetochron boundaries.

head plume triggered the rapid eruption of the Deccan basalt (e.g., White et al., 1987; White and McKenzie, 1989). Hooper (1990), however, argues for significant extension, and the subsequent rifting and separation, to have occurred after the development of the main Deccan province (see also Burke and Dewey, 1973; Richards et al., 1989), implying that impact of the plume head triggered melting directly. Sheth (1999, 2000, 2005) disputes the involvement of a plume altogether.

The earliest Deccan (68 Ma) manifestations were small-volume alkaline volcanic and intrusive rocks of the northern part of the province (Basu et al., 1993), which then progressed through to, and partially overlapped with, the younger and increasingly voluminous tholeiitic eruptives of the main Deccan province. Flood basalt magmatism began at 67 Ma in the Kutch–Narmada–Son rift valley area and progressed southwards, with the final flood eruptions occurring in the

early Paleocene (64 Ma) at the southern margin of the main Deccan province (Fig. 6; Mitchell and Widdowson, 1991; Widdowson et al., 2000). A final phase of rhyolitic, trachytic and basaltic Deccan volcanism occurred in the Bombay region at 62–64 Ma (Lightfoot et al., 1987; Sethna, 1999; Sheth et al., 2001), and was characterised by phreatomagmatic and spilitic-type eruptions occurring in a shallow, newly-formed brackish-marine gulf. This gulf had formed through marine incursion along the subsiding continental crust of the thinned Indian margin (Cripps et al., 2005) prior to the final separation of the Seychelles–Mascarene microcontinent at chron 27–28 (Todal and Eldholm, 1998); dredge samples reveal similar trachytic basalts capping foundered fault blocks on the conjugate Seychelles rift margin (Collier et al., 2004, 2005). Subsequently, magmatism moved offshore, across this thinned continental margin, and eventually onto newly-formed oceanic lithosphere to form the Chagos–Laccadive Ridge (Duncan and Hargreaves, 1990). Importantly, the onset of seafloor spreading along the Indian margin south of the offshore Cambay–Narmada–Son region began during chron 28, some 1–2 m.y. after the main Deccan province eruptive acme (Courtillot et al., 1988; Gallet et al., 1989; Chaubey et al., 1998; Todal and Eldholm, 1998).

Post-eruptive rifting of the Indian continental crust is further confirmed by the presence of extensive coast-parallel dyke swarms. These clearly cut through the upper part of the chron 29r Deccan succession (i.e., Bushe, Poladpur and Ambenali Formations, Fig. 5), indicating that coast-parallel extension must have occurred late in the development of the main Deccan province (Hooper, 1990). Moreover, the occurrence of Seychelles dykes (Devey and Stephens, 1991) of similar composition to the later, extrusive phases of the main Deccan province (i.e. Bushe Formation), similarly suggests that separation of the Seychelles–Mascarene microcontinent cannot have occurred prior to the main chron 29r eruptive acme. The fact that these lavas are amongst the most crustally contaminated of the entire Deccan succession (Cox and Hawkesworth, 1984; Devey and Lightfoot, 1986) further indicates that a significant thickness of Indian continental crust remained above the Deccan melting anomaly at this time.

The sedimentary record also aids in determining the chronology of the Seychelles rifting event. The offshore succession is typical of a rifted margin setting, and numerical modelling indicates an initial episode of rapid subsidence between 17°–20° N accompanied active extension of the margin during the period 60–63 Ma (Whiting et al., 1994). This offshore succession
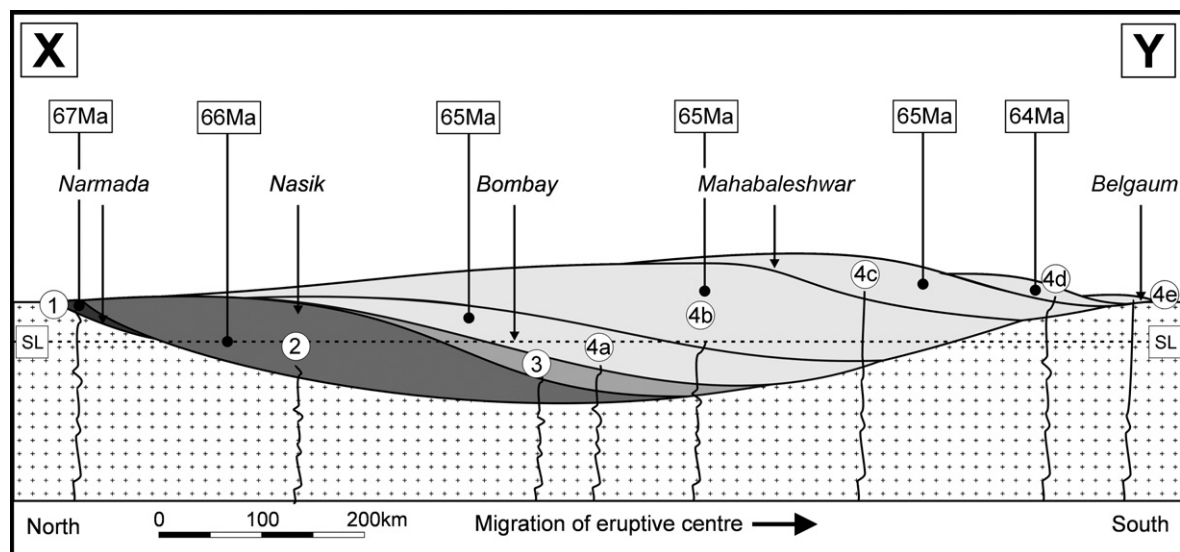
Fig. 6. North-south sketch section showing structure and stratigraphy of the Deccan lava succession along the Western Ghats escarpment 16°–22°N. Shading and numbering distinguish Kalsubai (2), Lonavala (3), and Wai (4) subgroups (Fig. 5). The Wai Subgroup is further divided into individual formation units Poladpur–Desur (4a–4e). Due to the northward movement of India over a hotspot source, successive eruptive packages (1–4e, dykes shown schematically) build on the southern flank of the evolving volcanic edifice. Vertical exaggeration ×25.

consists of a Paleocene early 'rift-fill' which was initially dominated by conglomerates and continental clastic sedimentation derived from the erosion of the main Deccan basalt succession and its adjacent basement lithologies; above these, progressively finer-grained shelfal clastics were deposited during later Paleocene times, eventually passing upward into late-Paleocene to Miocene marine carbonates, and then deeper water marine sediments (Whiting et al., 1994; Chaubey et al., 1998). The fact that the early 'rift-fill' sediments contain a substantial proportion of basalt-derived material illustrates three important facts: first, that the extensional topography forming the nascent continental margins was already undergoing uplift and erosion; second, that this erosion continued during the initial rifting event, and after the separation of the Seychelles–Mascarene microcontinent; and third, that the regions being denuded during the pre-rift extensional phase were already dominated by considerable thicknesses of Deccan lava fields.

Whilst there is strong evidence that the main phase of rifting leading to plate break-up began during the later stages, and culminated after, the volcanic activity of the main Deccan province, it is also apparent that lithospheric extension had been underway since at least the Maastrichtian in north-west peninsular India (Todal and Eldholm, 1998, and references therein). Arguably, this pre-break-up phase of extension and thinning could have controlled the location of eruption and composition

of the earlier magmas (Thompson and Gibson, 1991). Nevertheless, models invoking pre-Deccan rifting and separation remain difficult to explain geodynamically because isotopic data indicate that the majority of the subsequent Deccan magmatism was preferentially erupted through continental crust; clearly, if separation had indeed occurred prior to the main eruption of the Deccan Traps, then any magmatism would have more probably occurred at a locus where the asthenosphere had already reached the surface (i.e., through any coeval region of seafloor spreading along the nascent Indian margin). Such models would be inconsistent with current geochemical and isotopic data. Moreover, the apparent absence of any widespread seaward-dipping reflector sequences along the offshore western margin of India (Todal and Eldholm, 1998) is also inconsistent with rifting and separation having occurred prior to, or during, the main Deccan province volcanism.

To summarise this section, it would appear that bulk of the Deccan volcanism occurred before the main phase of plate break-up and the separation of the Seychelles–Mascarene microcontinent from India. However, the lithosphere extension that was to eventually culminate in this continental separation event had already begun in the Maastrichtian along inherited lines of weakness (Biswas, 1987). Accordingly, nascent extensional structures were probably beginning to evolve by the time of eruption of the main flood basalt volcanism (i.e., Late Maastrichtian to Paleocene).

5.2. Uplift associated with the Deccan province

Uplift associated with the Deccan Province can conveniently be divided in pre-, syn-, and -post-eruptive episodes. If the models of Griffiths and Campbell (1991) and Farnetani and Richards (1994) are correct for the Deccan, whereby a proto-plume head impacts on the base of the lithosphere and thins laterally, then the maximum transient uplift preceding the main Deccan province eruptive episode should have been in the Kutch–Cambay–western Narmada–Son rift valley region, with broadening but diminishing uplift further to the east and south (Fig. 4). Moreover, since the continued northward movement of India would have decoupled the site of initial plume head impact from the plume head centre, any initial thermal and dynamic of uplift in the northern areas would have been relatively short-lived. Seismic tomography identifies a cylindrical region of lower seismic velocities beneath central Kutch and the Cambay Rift. This has been interpreted as the position of the 'conduit' through which plume head material passed through the upper mantle before arriving at the base of the Indian lithosphere (Kennett and Widiyantoro, 1999).

The initial dynamic and thermal uplift effects above a putative Deccan plume would have been subsequently augmented by a wider magmatic underplating of the region. Underplating represents the un-erupted residue of a mantle melting event (Cox, 1993) and gabbroic bodies intruded into the crust which, together with the surface basalt eruption, serves to thicken the lithosphere (Maclennan and Lovell, 2002). This process is considered to be an important mechanism for driving regional syn-eruptive surface uplift and denudation of large continental areas (White and Lovell, 1997). Seismological evidence for Deccan-related underplating is found beneath the central and western regions of the Narmada–Son rift valley (Reddy et al., 1999).

Following eruption of the main Deccan basalts, and the Seychelles–Mascarene rifting event, erosion and eastward retreat of the Western Ghats escarpment has resulted in onshore denudational unloading, through the removal of 1–1.5 km thickness of Deccan basalt across the coastal plain (i.e. Konkan–Kanara lowlands) and the inner continental shelf (Widdowson and Gunnell, 1999). Onshore erosion and unloading has resulted in onshore, coast-parallel uplift, and concomitant offshore subsidence due to the depositional loading of the eroded materials. Subsequent isostatic adjustment has resulted in a lithospheric flexing of the entire margin (Widdowson, 1997); this post-eruptive onshore uplift is the origin of the coast-parallel anticlinal–monoclinal structure

developed in the basalt succession along the Western Ghats region of the Deccan province (Widdowson and Cox, 1996; Widdowson, 1997). Importantly, since denudational unloading is independent of thermal effects, it provides a long-term mechanism for generating permanent and continuing uplift (Gunnell et al., 2003) throughout the Cenozoic.

5.3. Sedimentation associated with regional uplift

5.3.1. Offshore Basin sedimentation (Kutch, Krishna–Godavari, and Cauvery basins)

The sedimentary records of the Kutch Basin of the north-west Indian coast (i.e. offshore of the western Narmada–Son rift valley), and the Krishna–Godavari and Cauvery Basins on the east coast (Fig. 4; inset) are all characterized by a three- to five-fold increase in the rate of sedimentation during the late Campanian to early Maastrichtian (Halkett et al., 2001). These all indicate an increase in denudation occurring in the continental hinterlands. The distribution of depositional facies in these basins also changed fundamentally during this interval because deeper marine sediments pass upward into shallow water facies and, eventually, fluvially-dominated clastic sedimentation, indicating rapid progradation of the proto-Godavari, Krishna and Cauvery river systems. This long-term shallowing cycle is at odds with the longer term late Campanian and early Maastrichtian eustatic sea-level change (Li et al., 2000; Adatte et al., 2002). It is also contrary to the pattern of deposition in contemporaneous Tethyan marine basins elsewhere (Goel et al., 1996). Accordingly, such comparisons effectively preclude long-term eustatic variation as the causative mechanism for the relative sea-level fall recorded in the offshore basins of Late Cretaceous India (Halkett, 2002). Moreover, subsidence analysis of well log data from Krishna–Godavari and Cauvery Basins shows several hundreds of metres of transient surface uplift from the Maastrichtian to the late Paleocene (Halkett et al., 2001). The timing of this transient uplift signal occurs at incrementally later intervals in the more southerly offshore basins (Halkett, 2002), and effectively parallels the southerly migration of volcanic activity observed in the construction of the Deccan Traps (Devey and Lightfoot, 1986; Mitchell and Widdowson, 1991; Fig. 6).

5.3.2. North-western main Deccan province (Western Narmada–Son Rift Valley and Cambay regions: earliest MDP eruptive phase; Fig. 4, area 1)

Cretaceous sediments of the intra-cratonic Narmada–Son rift succession have become locally deformed and

tilted (10°–20°), resulting in an angular unconformity. This is exposed in the western Narmada Valley where basal lava units (∼67 Ma) lie upon deformed Cretaceous sandstones. Late Cretaceous regional uplift and erosion is further evidenced in this area by local patches of conglomerate preserved between the western Narmada sedimentary succession and the overlying basalts; these conglomerates contain sub-rounded to sub-angular clasts of the underlying sandstones, lamprophyric dyke materials and, importantly, vesicular basalt. In addition, part of the later dyke swarm radiating from the Phenai Mata alkaline centre (∼68 Ma) cuts through both these conglomerates and the overlying basal lava flows, confirming that the clasts it contains were eroded during the earliest stages of Deccan volcanic activity.

The Late Cretaceous sedimentary history of this region is recorded by the deposition of the estuarine–fluviatile sandstones of the Nirmar sandstone, followed by a rapid and widespread transgression producing the Nodular and Coralline Limestones of the Bagh Group. These were followed by a marine regression, with the development of increasingly continental facies in the overlying Lameta Group. Importantly, this regional regression was contemporaneous with a global eustatic sea-level rise (Wignall, 2001; Adatte et al., 2002), indicating that NW India was undergoing significant tectonic uplift at this time. Such uplift also explains the increasingly continental-type sedimentation during deposition of the Lameta Group, and its continuing effects would then account for the local stripping of the early Deccan volcanic rocks and underlying Maastrichtian sedimentary rocks in the western Narmada region.

5.3.3. North-eastern main Deccan province (Eastern Narmada–Son Rift valley and Jabalpur and Mandla lobe areas: early to mid main Deccan province eruptive phase; Fig. 4, area 2)

In the eastern Narmada–Son Rift basin, the basement–basalt contact becomes well exposed in the hills around Jabalpur. Here, basement lithologies are covered with variable thicknesses of Maastrichtian terrigenous sediments and palaeosol horizons of the Lameta Group.

The basal Green Sandstone unit of the Lameta Group consists of quartz grains from the erosion of local granitic lithologies, but its green colour is imparted by clay (smectite) derived from the weathering and breakdown of basalt (Tandon et al., 1995; Salil et al., 1997). The rare earth element contents of the Green Sandstone and associated units further confirms significant clay-fraction (montmorillonite and and kaolinite) input derived from weathered Deccan basalt

(Salil and Shrivastava, 1996). The Green Sandstone is overlain by the lacustrine Lameta Group limestone which marks a change to semi-arid palustrine and lacustrine conditions, ephemeral lakes, widespread pedogenesis, and a significantly reduced clastic input. It is succeeded by the Mottled Nodular Beds which contain conglomeratic lag deposits interpreted as sheetwash deposits of a semi-arid alluvial plain (Tandon et al., 1995). These coarse sandstones and conglomeratic lags contain occasional sub-angular clasts of altered Deccan basalt.

At Jabalpur, this sedimentary succession is overlain and preserved by Ambenali and Mahabaleshwar Formation flow units (chron 29r/n; Fig. 4). However, earlier flows (Poladpur and Ambenali Formation) lie directly upon the basement rocks at lower elevations (Yedekar et al., 1996; Pattanayak and Shrivastava, 1999; Cripps, 2002), indicating that the region had already undergone several tens of metres of erosion and incision prior to the arrival of the first lava flows in this eastern region (Mandla Lobe) of the main Deccan province. Subsequent encroachment of the later lava units then filled this existing topography, and eventually capped the patches of late Maastrichtian, dinosaur-bearing Lameta Group that had remained preserved upon the higher, uneroded, elevations.

5.3.4. Eastern and south-eastern main Deccan province (Nagpur and Bidar areas: Poladpur to Mahabaleshwar formations; Fig. 4, area 3)

Elsewhere, in regions distal to active centres of volcanism in the western main Deccan province (i.e., Narmada–Nasik–Mumbai), there are thin sedimentary units (5–20 m) both immediately below, and intercalated within, the peripheral basalt succession. These indicate the existence of locally-restricted fluvial successions and shallow pseudo-marine lakes around the eastern and south-eastern margins of the Deccan province, during the Late Cretaceous and early Cenozoic (Mohabey et al., 1993; Prasad and Khajuria, 1995). A particularly large, shallow lake (∼700 km²), and surrounding expansive marshlands, developed in the Nand–Dongargaon Basin south of Nagpur (Mohabey and Samant, 2005). These lakes appear to have received a steady, fine-grained terrigenous input throughout the late Maastrichtian, indicating a sustained remoteness from co-existing regions of erosion occurring elsewhere.

The high nutrient supply to these lakes, as evidenced by phytoplankton blooms, was derived from the weathering and liberation of mobile elements from the Deccan volcanic succession developing far to the west (Samant and Mohabey, 2005), and supplied by

fluvial systems draining eastward across the land surface exposed around the fringes of the expanding lava fields (Cox, 1989). In many instances, patchy cross-bedded sandstone units cap and seal these lake successions, and represent an influx of coarser clastic material derived from the advancement, weathering and erosion of later Deccan lava fields. These lakes were eventually over-run during end-Maastrichtian to early Paleocene times by Wai Subgroup lavas, including the voluminous Poladpur and Ambenali Formations (chron 29r).

6. North Atlantic Igneous Province (NAIP) (∼62–54 Ma) (Stephen Jones)

The NAIP was emplaced during Paleocene–Eocene time across an area of several million square kilometres encompassing NW Europe, Greenland and Canada

(Fig. 7). Radiometric dating in combination with magnetostratigraphy indicates that the NAIP formed in two main phases (Saunders et al., 1997; Meyer et al., in press). Phase 1 took place within magnetic chron 26r (Selandian, ∼62–59 Ma) and includes intra-plate magmatism in the British Isles, SE and W Greenland, Baffin Island and possibly central E Greenland. Phase 2 began within magnetic chron 24r (Paleocene/Eocene transition, ∼56.5–54 Ma) and includes the volcanic passive margins between NW Europe and Greenland.

NAIP activity was accompanied by both transient and permanent uplift, and both were on the kilometre magnitude. A topographic reconstruction of the region prior to widespread uplift is given in Fig. 4 of Maclennan and Jones (2006). Pre-NAIP elevations ranged from several kilometres below sea-level to several kilometres above sea-level. Regional uplift was recorded by continuous deposition in areas that
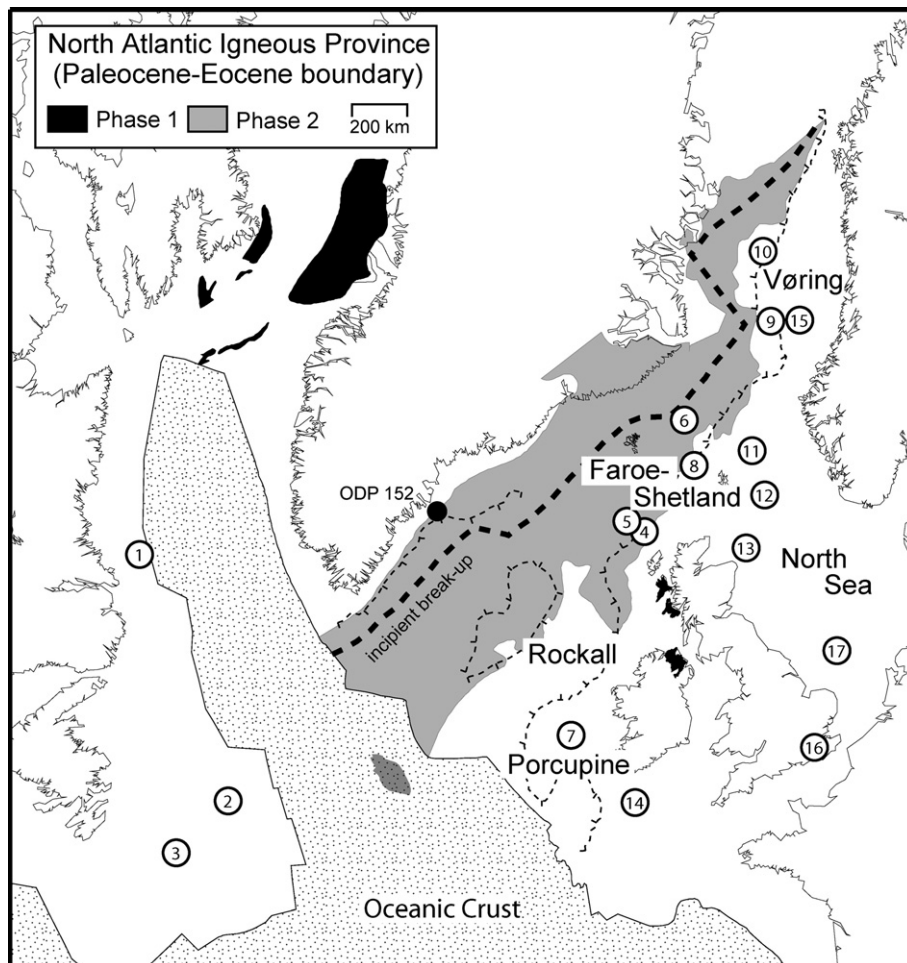
Fig. 7. North Atlantic tectonic reconstruction at Paleocene/Eocene boundary, immediately prior to Europe–Greenland break-up. Numbered circles mark locations of dynamic support estimates in Fig. 8f.

were originally deep marine environments, and by erosion in other areas. A large body of detailed work on NAIP vertical motions is concerned with quantifying permanent uplift and exhumation related to lower crustal igneous intrusions during both Phases 1 and 2 (Brodie and White, 1994, 1995; Barton and White, 1997; Rowley and White, 1998; Clift and Turner, 1998; Clift et al., 1998; Al-Kindi et al., 2003). Associated transient vertical motions have long been recognised, and recent efforts have been made to refine our knowledge of the timing and amplitude of these uplift events (Stewart, 1987; Milton et al., 1990; Nadin et al., 1997; Jones et al., 2001; Mackay et al., 2005). We concentrate here on reviewing the record of transient surface uplift since it is the easier to relate directly to mantle processes.

At present, the best records of transient uplift come from sedimentary basins surrounding the British Isles (Figs. 7 and 8). These basins contain near-complete Paleocene–Eocene successions that are among the most intensively studied in the North Atlantic, following decades of hydrocarbon exploration. One group of dynamic support estimates has been determined from backstripped subsidence histories of extensional sedimentary basins. More detailed histories of relative sea-level change have been reconstructed from indicators such as the height of delta foreset clinoforms, the elevation of the delta topsets with respect to the basin margin, and the relief of subaerially incised valleys. The British and Irish offshore basins are ideally situated to record uplift associated with the British Paleocene Igneous Province (BPIP), part of NAIP Phase 1. However, we shall see that uplift associated with the BPIP was minor and localised, while major and widespread uplift was associated with NAIP Phase 2. Models of mantle circulation to explain the NAIP have hitherto been based mainly on the igneous record. The contrast between uplift responses to the two igneous phases provides important new constraints on these models.

6.1. Transient uplift associated with NAIP Phase 1

During the Danian and Selandian, prior to and coeval with igneous Phase 1, delta plain deposits were restricted to a narrow strip at high elevation along the basin margins (Shannon et al., 1993; Reynolds, 1994; Ebdon et al., 1995). These deltaic deposits are often missing by erosion following major uplift during the Thanetian. The high elevation and limited areal extent of Danian–Selandian delta plain deposits imply high relative sea-level. Most Danian–Selandian sediment is contained in basin floor fans. Both the accumulation rate and the proportion of sand in these fans increased into

the Selandian (Reynolds, 1994; Ebdon et al., 1995; Jones et al., 2001). Increase in flux of sandy sediment without a major coeval drop in sea-level in the basins themselves is best interpreted as a response to localised uplift of the sediment source region, which includes the BPIP. The idea of localised uplift is reinforced by the observation that Selandian sediment accumulation rates are highest in the Faroe–Shetland Basin, immediately adjacent to the BPIP, and progressively lower in the North Sea and Porcupine Basins, each situated further from the BPIP. Only lower bounds on uplift are available within the outcrop of the BPIP because uplift led to denudation. Estimates of depositional water depth for Upper Cretaceous limestones in Northern Ireland mean that uplift of at least 400 m is required to explain the karstic erosion surface developed beneath the plateau lavas (Jones, 2000). A component of this uplift was permanent (Brodie and White, 1995; Rowley and White, 1998). In contrast, basins surrounding the British Isles suffered uplift of no more than 200 m prior to the Thanetian, and the greater part of this uplift was probably transient (Milton et al., 1990; Jones et al., 2001; Smallwood and Gill, 2002).

6.2. Transient uplift associated with NAIP Phase 2

The greater part of the total Paleocene–Eocene transient uplift that affected the British Isles occurred during the Thanetian, prior to and during NAIP Phase 2 (Fig. 8). The main indicators of uplift are that deltaic deposits stepped progressively outward and downward into all the surrounding basins, and that the basin margins underwent sub aerial erosion (Jones and Milton, 1994; Reynolds, 1994; Smallwood and Gill, 2002; Jones et al., 2001). Simultaneously, sediment flux into all basins increased (Liu and Galloway, 1997; Jones et al., 2001), although the sand/mud ratio in the deep-water sediment fans decreased as the sand component became trapped in marginal delta complexes (Reynolds, 1994). Peak uplift occurred just before the Paleocene/Eocene boundary (55.8 Ma) (Maclennan and Jones, 2006). The detailed geometries of the deltaic sediments in each basin provide a detailed uplift record. In the Faroe–Shetland Basin, heights of the delta foreset clinoforms decreased from 500 m to 300 m during main part of the Thanetian, indicating gradual shallowing. During the latest Thanetian, peak uplift caused development of a regional subareal erosion surface incised by river valleys up to 200 m deep (Fig. 8a). Transition from 500 m-high submarine clinoforms to 200 m-deep sub aerial valleys indicates at least 700 m of transient uplift through the Thanetian (Fig. 8e). In the North Sea, the delta plain

stepped downwards into the basin, indicating several hundred metres of uplift (Fig. 8b). In the Porcupine Basin, a wedge of sediment prograded rapidly into the basin during the Late Paleocene (Shannon et al., 1993; Jones et al., 2001). In SE England, uplift of around 100 m after deposition of the marine Thanet Sand Formation during the Late Paleocene lead to development of an erosional unconformity before deposition of the Upnor
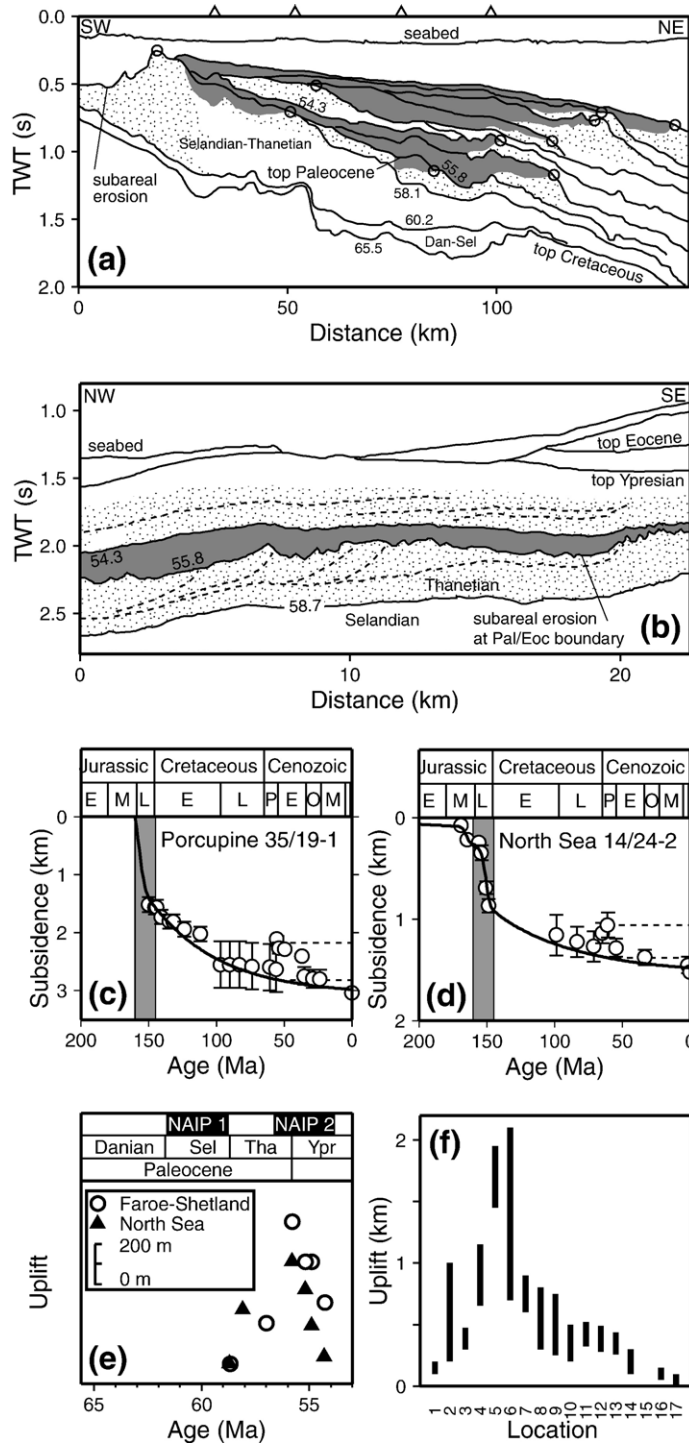
Formation in coastal conditions close to the Paleocene/Eocene boundary (Knox, 1998).

Following peak transient uplift close to the Paleocene/Eocene boundary, regional subsidence occurred through the Early Eocene. In the Faroe–Shetland Basin, delta top deposits accumulated close to sea-level during the earliest Ypresian, and middle Ypresian clinoforms indicate water depths of 250 m. In the northern North Sea, delta topsets first stepped upward and toward the basin margin, before aggrading and prograding as water depths continued to deepen. A similar geometry occurred in the Porcupine Basin, where the increasing height of Ypresian delta clinoforms indicates several hundred metres of sea-level rise (Jones et al., 2001). Sedimentological and biostratigraphical studies of the onshore section in SE England also record transgression (Knox, 1998). Eocene subsidence rates were more rapid than anticipated rates of post-rift thermal subsidence, and total Eocene subsidence was roughly equal to the Paleocene uplift in each of these basins, indicating that subsidence resulted from decay of the Paleocene transient uplift by withdrawal of dynamic support (Nadin et al., 1997; Jones et al., 2001).

Complementary estimates of transient uplift have been derived from the subsidence histories of extensional sedimentary basins. The evolution of extensional basins is well understood (McKenzie, 1978), allowing the post-rift subsidence history to be predicted when the syn-rift subsidence history is known. Discrepancy between the observed and model subsidence curves can be interpreted in terms of regional dynamic support, provided that global sea-level change or significant coeval plate stretching or shortening can be ruled out. Observed subsidence curves can be calculated from 1D well sections or 2D interpreted stratigraphic profiles using the standard backstripping technique. The advantage of the backstripping method over inferring uplift/subsidence directly from geological indicators of sea-level change is that backstripping takes full account of subsidence caused by sediment accumulation and compaction, tectonic basin subsidence and global sea-level change.

Published estimates of total Paleocene transient uplift, determined from North Atlantic basins, range from less than 100 m in the southern North Sea, to 1–2 km in

the Rockall Trough (Fig. 8f). These suggest that, at the time of the Paleocene/Eocene boundary, the region of the British Isles sat on the southeastern quadrant of a larger uplifted swell. Information from other basins on the European, Greenland and Canadian continental margins, though less detailed and often from incomplete eroded sections, is compatible with this view. Unconformities developed in response to Paleocene/Eocene boundary uplift in the Jeanne d'Arc and Orphan Basins, offshore Newfoundland (Deptuck et al., 2003), the Vøring Basin, offshore Norway (Ren et al., 1998) and at Kangerdlugssuaq, East and West Greenland (Clift et al., 1998; Dam et al., 1998). Simple models of the regional dynamically supported swell based on the collated uplift estimates in Fig. 8f can be found in Maclennan and Jones (2006).

6.3. Smaller scale uplift/subsidence cycles

Superimposed on the long-term Paleocene–Early Eocene uplift-subsidence cycle were a number of uplift/subsidence phases of shorter duration and smaller amplitude (Mudge and Jones, 2004). The most important single phase of uplift occurred during the latest Paleocene, immediately before peak uplift at the Paleocene/Eocene boundary. In the Faroe–Shetland Basin, the sedimentary architecture shows that 500 m of permanent uplift occurred during this phase, while total transient uplift is estimated at 400–900 m using backstripping (Fig. 8). Hence the latest Paleocene event accounts for more than half of the total uplift in the Faroe–Shetland Basin. In the North Sea, comparison of uplift estimates from sedimentary architecture (Jones and Milton, 1994) and subsidence analysis (Nadin et al., 1997; Mackay et al., 2005) suggests the same conclusion (Jones et al., 2001).

An important characteristic of all the short-term uplift phases is the short time-interval between onset of uplift and peak uplift. A good illustration is provided by the stratigraphy of Northern Ireland, where several tens of metres of Upper Cretaceous marine limestone was removed by subaerial erosion before extrusion of plateau lavas belonging to NAIP Phase 1. Assuming reasonable limestone erosion rates, the time interval between emergence of the limestone surface and eruption of the first

Fig. 8. Examples of stratigraphic data used for measuring uplift around the British Isles. (a) and (b) line drawings of seismic reflection profiles from North Sea and Faroe–Shetland Basin (after Jones and Milton, 1994; Smallwood and Gill, 2002). Grey shading, delta topset deposits; stippled regions, delta foreset deposits. Stratigraphy after Mudge and Jones (2004); numbers are ages in m.y. Circles in (a) are shelf-slope breaks used to construct sea-level curve in (e). Sections located close to 13 and 8, Fig. 7. (c) and (d) backstripped basement subsidence histories from Porcupine Basin and North Sea, located close to 7 and 13, respectively, on Fig. 1. Circles: observed backstripped subsidence (error bars represent uncertainty in depositional water depth); lines: model subsidence curve constrained by observed syn-rift subsidence; shaded regions: syn-rift period determined from seismic images of faulting. Data after Jones and White (2003). (e) Summary of relative sea-level change information derived from (a) and (b). (f) Summary of peak dynamic support estimates from published backstripping studies (Nadin et al., 1997; Jones et al., 2001; Mackay et al., 2005; Ceramicola et al., 2005).

basalt flows was less than 1 m.y., and was possibly of the order of 10 k.y. (Simms, 2000). A short duration is also estimated for the major phase of latest Paleocene uplift that preceded peak uplift. The detailed stratigraphic framework developed for the Faroe–Shetland and North Sea Basins suggests that, once again, onset of uplift was at most 1 m.y. and more likely a few 100 k.y. or less before the peak in uplift (Clift et al., 1998; Mudge and Jones, 2004). More detailed discussion concerning the rapid timescales of uplift can be found in Maclennan and Jones (2006).

6.4. Summary of NAIP vertical motions

Several new and important conclusions concerning the timing and spatial distribution of regional uplift arise from this summary. Patterns of uplift associated with Phases 1 and 2 of NAIP activity were different. Uplift associated with igneous Phase 1 was minor (hundreds of metres) and was localised within a few hundred kilometres of the igneous outcrops. Uplift associated with Phase 2 was several thousand kilometres in diameter and up to 2 km in amplitude (Ceramicola et al., 2005). Peak regional uplift occurred just before the Paleocene/Eocene boundary (55.8 Ma), coeval with NAIP Phase 2 and continental break-up between NW Europe and Greenland. It also coincided with the Paleocene/Eocene rapid and extreme global climate change event. Higher order uplift/subsidence cycles were superimposed upon the long-term Paleocene–Eocene uplift/subsidence cycle. The uplift phase of each short-term cycle was rapid, probably occurring in less than 1 m.y. and possibly over a period as short as 10 k.y. to 100 k.y. (White and Lovell, 1997) These observations place important constraints on any models for the underlying mantle-driven mechanisms.

7. Yellowstone Province (~16–0 Ma) (Ken Pierce and Lisa Morgan)

Jason Morgan (1972) postulated that the Yellowstone-Snake River Plain volcanism represented a hotspot track, and Armstrong et al. (1975) showed that the initiation of rhyolitic volcanism along this track is systematically younger towards Yellowstone (Fig. 9). A vigorous debate has ensued as to whether or not this volcanic progression results from a mantle plume beneath the southwest-moving North American plate. For pro-plume arguments, the reader is referred to Suppe et al. (1975), Anders et al. (1989), Westaway (1989), Pierce and Morgan (1992), Smith and Braile (1993), Camp (1995), Takahahshi et al. (1998), Pierce et al. (2002), Camp and Ross (2004),

Morgan et al. (2005) and Hooper et al. (in press). For non-plume arguments, see Hamilton (2003), Humphreys et al. (2000) and Christiansen et al. (2002).

Recently, two seismic tomography studies identified a low-velocity mantle anomaly, considered to be a thermal plume, inclined to the northwest from Yellowstone at ~20° from vertical and extending to a depth of about 500 km (Yuan and Dueker, 2005; Waite et al., 2006). A relation may exist between the inferred plume and the asymmetric pattern of faulting, uplift, and recent basaltic volcanism. The pattern of faulting and uplift associated with the Yellowstone hotspot track (Fig. 10) flares outward ~1.6 times farther to the south than to the north (Pierce and Morgan, 2005). Both this asymmetry and the southeast upward rise of the Yellowstone plume might be explained by upper mantle flow as modeled to the east (Steinberger, 2000) or most concordantly to the southeast (Berkeley model, Bernhard Steinberger, written comm., 2005). Upward leakage from an inclined plume might also be responsible for the concentration of basaltic vents, basaltic rifts zones, and still-active faults along the northern part of the hotspot track.

Geologic interpretation of the continental setting of the Yellowstone-Snake River Plain volcanic province is complicated by a long history of deformation, erosion, and sedimentation. The later part of this geologic history includes compressional tectonics of both the Sevier (late Mesozoic) and Laramide orogenies (Cretaceous–Neogene). A local change to extensional graben formation and andesitic volcanism occurred north of the hotspot track in Eocene time (Janecke et al., 1997). For the larger Rocky Mountain region, sediment accumulation indicates basin subsidence from about 35 Ma to between 8 and 4 Ma, followed by Rocky Mountain "Plateau" uplift and incision (McMillan et al., 2006). West of the Rocky Mountains, modern Basin-and-Range tectonics was underway by ~15 Ma in mid-Miocene time, with east-west extension creating north-trending basins and ranges (Christiansen and Yeats, 1992).

The Yellowstone hotspot created a volcanic track that started in the central part of the Basin and Range, and progressed 700 km northeast to the present-day Yellowstone Plateau (Fig. 9). The start of the track at about 16 Ma is characterized by extensive and widespread rhyolitic volcanism in the central and southern part of the Basin and Range and coeval basaltic volcanism associated with the Columbia River Basalt and similar flood basalt provinces in Oregon and California (Fig. 9). About 95% of the estimated volume of 220,000 km^3 of Columbia River and Oregon Plateau basalts were erupted within a 2 m.y. interval (Carson and Hart, 1988; Tolan et al., 1989; Baksi, 1990). The CRB and related basalts were emplaced

through thin Mesozoic oceanic crust, whereas the 14–17 Ma rhyolites of the hotspot track were generated above thicker and more silicic crust (Draper, 1991; Pierce et al., 2002; Camp and Ross, 2004). The basalt versus rhyolite dichotomy can be attributed to these contrasting crustal compositions that are delineated by the $^{87}Sr/^{86}Sr$ 0.706 and 0.704 contours (Fig. 9).

The continuity of the Yellowstone hotspot track from its present position at Yellowstone back in time to an apparent start with extensive volcanism in Nevada, Oregon, and Washington conforms to the plume head/plume tail model proposed by Richards et al. (1989). A voluminous plume head that pancaked outward to a radius of 500–1000 km at the base of the North American plate has been invoked to explain the initial large area of volcanism (Pierce and Morgan, 1990; Draper, 1991; Pierce and Morgan, 1992; Camp, 1995; Takahahshi et al., 1998; Pierce et al., 2002; Camp and Ross, 2004; Jordan et al., 2004). Later volcanism was much more restricted and aligned along the hotspot track (Fig. 9), possibly because the magmatism was associated with a narrow plume 'tail'.

The 16–14 Ma basaltic and rhyolitic volcanism associated with the inferred plume head is distributed
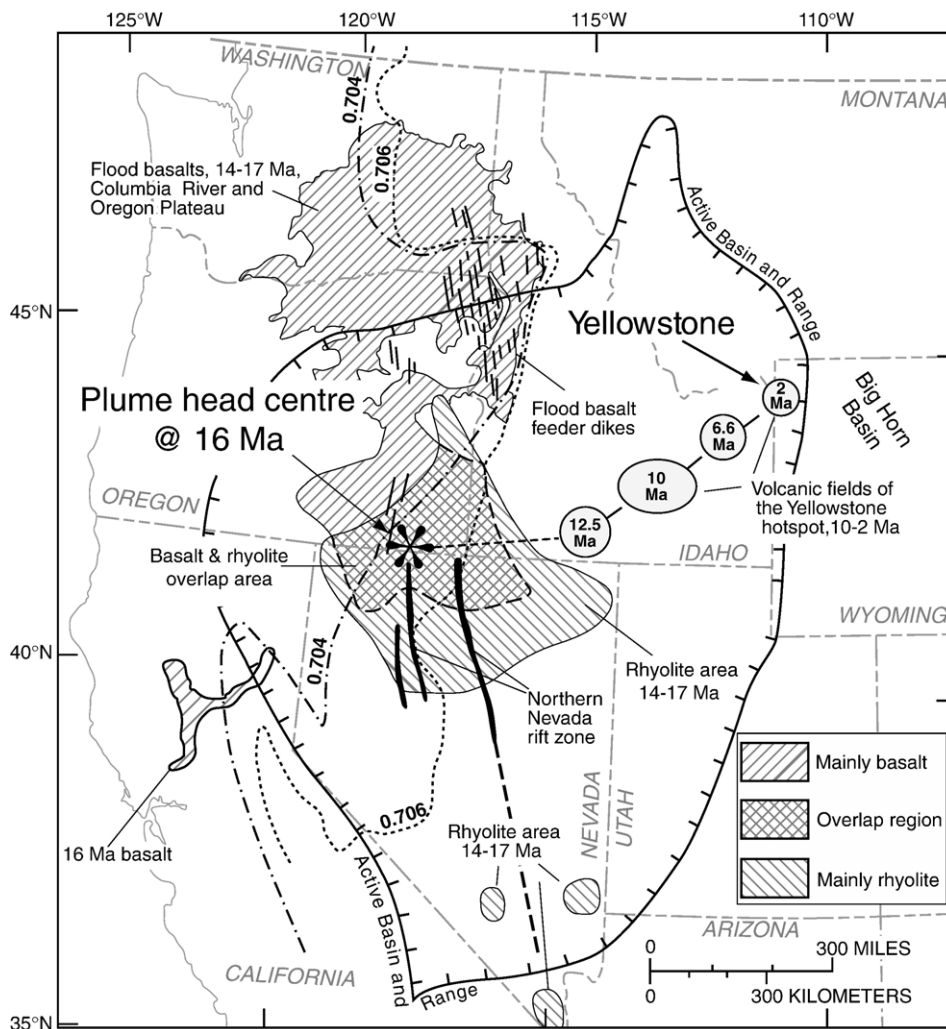
Fig. 9. Map of the western United States showing the track of the Yellowstone hotspot (after Pierce and Morgan, 1992). The track starts ∼ 16 Ma with widespread volcanism inferred to result from a plume head rising beneath the North American Plate. Such a plume head produced flood basalts to the north overlapping with rhyolites to the south associated respectively with Mesozoic oceanic crust and a Palaeozoic and older crust. Later, hotspot volcanism forms a narrow, focused track with volcanic fields starting at 10.2 Ma, 6.65, and 2.05 Ma. These fields progress north 55°E at 29 km per million years (not adjusted for tectonic extension), and are inferred to represent a plume tail phase.

over a large area (Fig. 9). In contrast, the 10 Ma and younger rhyolitic fields form a linear progression attributed to a plume tail leaving a track migrating N 55° E at about 29 km/m.y. that creates the well-defined 90-km-wide topographic trench of the eastern Snake River Plain.
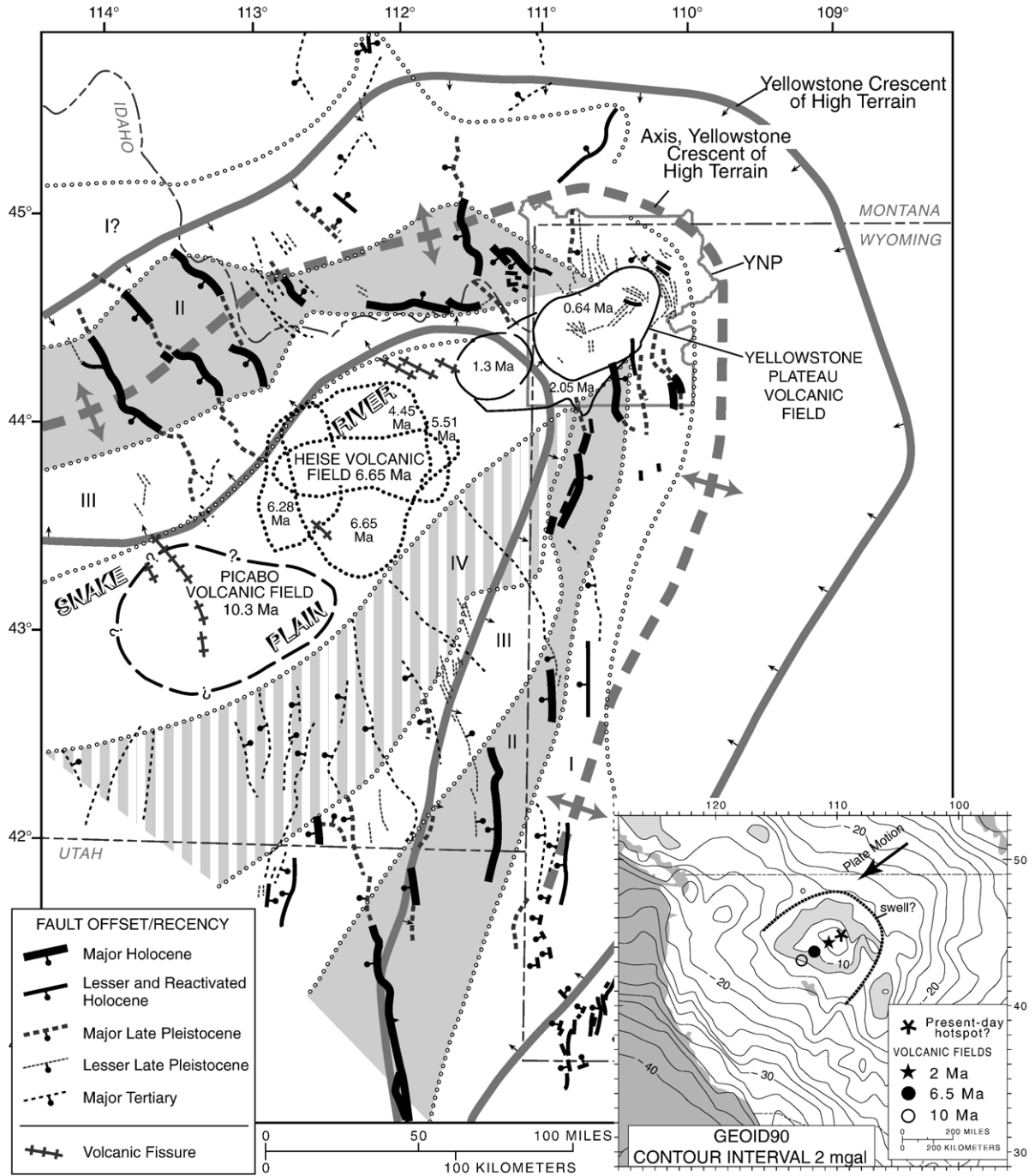
Fig. 10. Map of 10 Ma and younger part of the Yellowstone hotspot track (from Pierce and Morgan, 1992). Volcanic fields become younger to the northeast at a rate similar to the southwesterly-motion of the North American Plate. Late Cenozoic faults (black lines) are subdivided by recency of activity and range-front relief, the heavier lines being the most active. Faulting is subdivided into belts I, II, III, and IV, and that are separated by open-circle lines. The Yellowstone crescent of high terrain is outlined by the continuous grey line, and the axis of the crescent is indicated by the dashed grey line. Inset map shows geoid of the western U.S. (Milbert, 1991).

7.1. The key evidence for uplift

Several observations are well explained by plume-related uplift. The Yellowstone area stands high on the western North American plate and supports the Continental Divide. The axis of the Yellowstone Crescent of High Terrain, outlined by the wide grey line in Fig. 10, flares out in a "bow wave"-like pattern outward from the northeast progression of hotspot volcanism. This Crescent forms an arc that crests ahead (NE) of the youngest volcanism of the hotspot track. High mountain areas in this Crescent near the east boundary of Yellowstone National Park are formed of weakly consolidated, erodible bedrock of the Eocene Absaroka Volcanic Supergroup. There, a gently rolling upland above treeline is sharply incised by steep valleys a kilometre deep. Prior to the cutting of the modern canyons, 3.5-Ma basalt was erupted onto this surface. This incision can be explained by ongoing rock uplift (Pierce and Morgan, 1992). Additional evidence for young uplift and incision can be seen along the southeast and northwest part of the Crescent near the borders of Yellowstone National Park, where readily erodible bedrock of Mesozoic shales and sandstones form high mountains (Pierce and Morgan, 1992). Smith and Braile (1993) conclude that a 650 m topographic transient high centres on Yellowstone.

The highest part of the geoid in the United States coincides with the present position of the Yellowstone hotspot (Fig. 10, inset map). This US geoid culmination on Yellowstone contrasts with both the US Bouguer gravity and topography that culminate in western Colorado, with Yellowstone having a lesser anomaly. "Geoid anomalies reveal deep isostatic compensation. The geoid height of an isostatically compensated region is proportional to the elevation times the depth of compensation. The Bouguer gravity anomaly of a broad feature is proportional to elevation." (Norman Sleep, written commun., 2006). No geologic process other than the Yellowstone plume explains the geoid anomaly centered on Yellowstone, and explanation of this anomaly favours a young, deep, ongoing process beneath Yellowstone. Lowry et al. (2000) conclude that "The largest of the significant dynamic elevation anomalies [in the western U.S.] is consistent with that predicted by numerical modelling of the Yellowstone hotspot swell."

Molnar and England (1990a,b) present substantial arguments that late Cenozoic incision results from ice-age climates rather than non-isostatic uplift. Molnar and England (1990a) examine the geophysical basis of uplift and question ongoing rapid uplift distinct from isostatic uplift associated with accelerated erosion. However, if mantle plumes exist, then a real, deep-seated uplift process may exist (Şengör, 2001; Pierce et al., 2002).

Two well-dated Quaternary terraces along the Wind River in Wyoming, approximately 200 km SE of Yellowstone, indicate tilting away from the Yellowstone
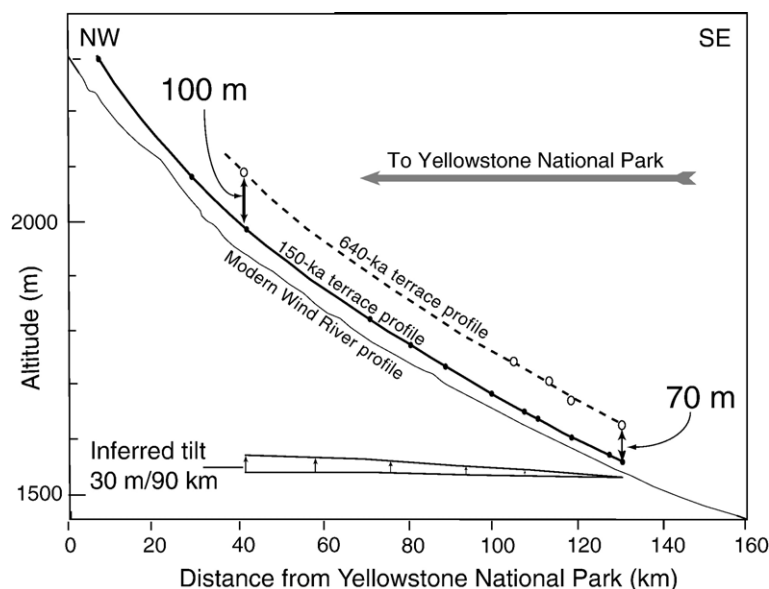
Fig. 11. Profiles of two dated terraces along the Wind River south of Yellowstone that diverge upstream towards the Yellowstone hotspot (after Jaworowski, 1994). Over a distance of 90 km towards Yellowstone, the higher, 0.5 m.y.-older terrace increases in height above a lower terrace by 30 m compatible with uplift associated with the Yellowstone hotspot.

area (Figs. 10 and 11). Over a distance of 90 km, a 640-k.y. terrace increases 30 m more in height towards Yellowstone than does a 150-k.y. terrace. Lava Creek ash dates the 640-k.y. terrace (Jaworowski, 1994) and the 150-k.y. terrace is dated by U-series ages (Sharp et al., 2003). These two terraces thus span an interval of ∼ 0.5 m.y. Such tilting across a geoid anomaly with an inferred uplift radius of 200 km (Fig. 10, inset) yields an uplift longevity of ∼ 8 m.y. (200 km at the North American plate rate of 25 km/m.y.). Assuming a straight-lever geometry of uplift, these dimensions compute to ∼ 1000 m total hotspot uplift (30 m × 16 {8 m.y./0.5 m.y.} × 2.2 {200 km/90 km} = 1056 m). A kilometre of uplift over 8 m.y. yields an uplift rate of ∼ 0.13 mm/yr.

East of Yellowstone, terraces in the Bighorn Basin are tilted away from Yellowstone such that streams flowing away from the Yellowstone have terraces that diverge upstream (to the west), whereas streams flowing towards Yellowstone have terraces that converge upstream (to the east) (Pierce and Morgan, 1992). Migration patterns of streams in the Bighorn Basin east of Yellowstone on the leading margin of hotspot deformation form terrace flights that step down eastward in a manner which is consistent with tilting away from Yellowstone (Pierce and Morgan, 1992). In addition, adjacent terrace profiles on Rock Creek on the northeastern edge of Yellowstone (Fig. 10) show a downstream convergence/divergence pattern indicating that through time the location of convergence/divergence has migrated away from Yellowstone (Pierce and Morgan, 1992).

Contrasts in the relative extent of glaciers at about 140 ka and 20 ka in the region are consistent with uplift on the leading margin of the Yellowstone Crescent of High Terrain and subsidence on the trailing margin (Fig. 10) (Pierce and Morgan, 1992). On the trailing margin, 140-ka moraines extend way beyond 20-ka moraines. On the leading, uplifting slope of the Crescent of High Terrain, the ratio of the length of last glaciation to penultimate glaciation estimated using glacier length and snowline change, yields an uplift rate of ∼ 0.15 to ∼ 0.4 mm/yr (Pierce and Morgan, 1992).

Mapping by Christiansen (2001) of the 2.05-Ma Huckleberry Ridge Tuff shows that near the crest of the Yellowstone Crescent of High Terrain, the ignimbrite occurs 500 m to 1000 m above the altitude of its source caldera (Pierce and Morgan, 1992). These high exposures of 2.05-Ma ignimbrite to the north and east of its source caldera indicate uplift on the leading northern and eastern margin of the hotspot, in contrast to exposures of the ignimbrite to the south and west where it is at similar altitudes as the source caldera.

7.2. Timing of uplift, in relation to the timing of any rifting and magmatism

The leading margin of the Yellowstone Crescent of High Terrain is 100 km northeast of, and in advance of, the progression of hotspot magmatism. Similarly, the geoid anomaly has an outer margin 200–250 km northeast of and in advance of Yellowstone volcanism (Fig. 10).

Quaternary basaltic magmatism of the eastern Snake River Plain occurs on rifts trending at a high angle to the margins of the plain and the hotspot track (Fig. 10). Additionally, extensional faulting of Basin and Range mountains adjacent to the hotspot track is also at a high angle to the track (Fig. 10; Pierce and Morgan, 1992; Waite and Smith, 2002). This extension direction is at nearly right angles to that expected if the eastern Snake River Plain were a rift zone, as suggested by Hamilton (2003).

The belt of faulting that extends south from the Yellowstone Plateau is restricted to the inner subsiding slope of the Yellowstone Crescent of High Terrain (Fig. 10), consistent with gravity-driven extension on the inner slope. In contrast, faulting is absent or minor farther east, consistent with compression (or non-extension) as the North American plate moves S55°W over the hump represented by the geoid high. The Continental Divide appears to have migrated northeastward in conjunction with movement of the Yellowstone hotspot (Pierce et al., 2002) in part based on mollusc biogeography (Taylor and Bright, 1987) and Miocene drainage basins (Wood and Clemens, 2002).

For the Columbia River flood basalts, northward offlap of basalt units with time is shown by Camp (1995) to reflect south to north migration of uplift, with local uplift rates of about 2 to 3 mm/year. Other indicators of uplift in this inferred plume head area include leaf-morphology studies and orographic precipitation patterns as summarized by Pierce et al. (2002).

7.3. The scale and extent of the uplift

The hotspot track is 700 km long and started about at 16 Ma. We propose that the horizontal scale of the Yellowstone hotspot disturbance, as described by its identifying surficial processes of volcanism, faulting, and uplift, is driven by processes of compatible scale at depth. At the start of the hotspot track ∼ 16–14 Ma, combined flood-basalt volcanism and rhyolitic volcanism is extensive over a north-south distance of more than 900 km (Pierce et al., 2002, Figs. 1 and 5).

For the modern Yellowstone hotspot, some horizontal dimensions are: (1) the Crescent of High Terrain is ∼ 400 km across, (2) the belts of faulting west and south

of the Yellowstone flare outward to ∼400 km, measured perpendicular to the hotspot track, and (3) the geoid anomaly, measured perpendicular to the hotspot track, is ∼700 km across. Surface uplift of roughly a kilometre is associated with the current Yellowstone hotspot. The tilting of the Wind River terraces extrapolates to about 1 km of uplift over the last ∼8 m.y or an uplift rate of ∼0.1 mm/yr. The 2.05-Ma Huckleberry Ridge Tuff occurs 500 m to 1,000 m higher near the crest of the Crescent of High Terrain than it is at its source. Glacier length ratios on the leading half of the Crescent of High Terrain indicate uplift rates of ∼0.15 to ∼0.4 mm/yr (Pierce and Morgan, 1992). Thus, the hotspot history indicates a sustained, large-scale process on a scale of many hundreds of km across at the surface and comparable scale at depth, that has been active over the last 16 m.y.

8. Discussion

All five LIP case studies presented here are associated with surface uplift. In this section, we first summarise the most important observations of uplift, rifting and magmatism from individual provinces. One interesting aspect of this comparison is the wide variation in preservation of the uplift signal in the geological record. This variation results from interplay between spatially varying pre-uplift palaeogeography and spatially varying transient surface uplift. We then discuss problems with both non-plume and plume models using examples from the five case studies. There are major problems with non-plume models, but there are also problems with some starting-plume models.

8.1. Key points from individual provinces

The Emeishan Province provides the best opportunity to test whether accompanying surface uplift had a roughly circular planform and domal cross-section, as predicted by some starting plume models. Surface uplift is interpreted from erosion of limestones that underlie the basalts, which comprise a regionally extensive record despite incomplete preservation of the LIP itself. The erosional record can be interpreted directly in terms of uplift because a broad, shallow water carbonate platform covered the area prior to LIP emplacement, so that pre-uplift topography and sediment accumulation are well constrained. Stratigraphic thinning and the isopachs of the Maokou Formation outline a subcircular region (Fig. 1), strongly indicating that long-wavelength (about 1600 km in diameter) domal uplift occurred before the eruption of the Emeishan basalts. Detailed biostratigra-

phy established for the limestones shows that uplift began less than 2.5 m.y. before the eruption of the basalts.

A component of the rapid, pre-volcanic domal surface uplift was transient and probably represents dynamic support. However, persistent crustal elevation in the "Chuandian old land" (at the centre of the eroded region) over at least 45 m.y. implies permanent surface uplift that is more easily explained by magmatic underplating of the crust. Supporting evidence for magmatic underplating in the Emeishan LIP comes from recent seismic tomographic data, which reveal a high velocity lower crust ($Vp=7.1$–7.8 km/s) about 20 km thick in the west Yangtze Craton (Liu et al., 2001). This high velocity lower crust likely represents emplacement of picritic magmas at the crust-mantle boundary (Xu et al., 2003, 2004) due to the density contrast between primary magmas and crust (Cox, 1980).

The amount and extent of surface uplift associated with Siberian Trap magmatism are far less clear. Because large parts of the Trap region are deeply buried beneath the West Siberian Basin, it is not yet possible to map erosion or surface uplift across the entire province, as it is in the Emeishan and North Atlantic Provinces. On the Siberian craton, where the sedimentary record is most complete, there is little evidence for either pre-volcanic or syn-volcanic uplift and erosion, and indeed there may even have been slight subsidence in some locations during these periods (Czamanske et al., 1998). However, the sedimentary sequences on the thick, stable craton do not provide the full picture. The absence of Permian strata beneath large tracts of the West Siberian Basin suggests that significant pre-volcanic uplift may have occurred there, although the magnitude and detailed timing are not yet constrained.

The West Siberian Basin and Khatanga Trough appear to have formed by rifting. Rifting probably began before magmatism and certainly continued after the traps had been emplaced. Rifting may have controlled the eruption sites of the basalts, but it is not clear whether rifting alone triggered magma formation or whether rifting-related decompression alone can account for the observed volume and composition of basalt. On one hand, a wideangle seismic profile shows that the crust immediately adjacent to the Siberian Craton was thinned by a factor of 3 to 4, and images a high velocity crustal body that could represent igneous underplating following decompressional melting (Pavlenkova et al., 2002). This rifting might explain the volume of Siberian Traps magmatism, provided that the duration of rifting was less than a few million years and the asthenosphere was at least 100 °C hotter than normal (Bown and White, 1995). On the other hand, stretching estimates from

subsidence analyses from other parts of the basin are too small to generate enough shallow decompressional melting (Saunders et al., 2005). With these uncertainties, it is not yet possible to state unequivocally that a mantle plume was involved in the formation of the Siberian Traps. However, given the large energy requirements for the formation of the basalts, a plume model still seems the most plausible working hypothesis.

The regional structural configuration in the Deccan Province is similar to that of the Siberian Traps, in that the basalts cover both a cratonic platform (the Indian subcontinent) and are also found in an adjacent offshore rift basin related to continental break-up between India and the Seychelles microcontinent. In the Deccan, the sediment–basalt contact records widespread regional uplift and erosion of the Indian Platform, whereas little uplift affected the Siberian Craton. High velocity lower crustal bodies in the offshore part of the Deccan province, and seaward-dipping reflectors on the Sey-chelles conjugate margin, have been interpreted as syn-rift intrusive and extrusive igneous activity respectively (Coffin and Eldholm, 1994; Collier et al., 2004, 2005), and thus confirm a link between LIP magmatism and rifting. However, since the main phase of coast parallel dyke emplacement along the Indian margin post-dates much of the main (chron 29r) Deccan succession, the main phase of lithosphere extension must have occurred late in the eruptive episode. Final continental separation between India and the Seychelles did not occur until mid chron 27–28 time (64–62 Ma) (Todal and Eldholm, 1998; Collier et al., 2004, 2005), some 1 to 2 m.y. after the main pulse of Decan LIP activity; onshore, relatively minor rifting and dyke emplacement (Widdowson et al., 2000) continued until this time.

Detailed mapping of the Deccan sediment–basalt contact, and the palaeosurfaces on basalt flows, show how the location of magmatism and erosion migrated southward through time. Subsidence histories of sedimentary basins offshore west and east of India indicate that a component of the surface uplift was both widespread and transient. Interpretation of sedimentary successions in both offshore and onshore basins show that regional regression caused by this transient uplift began in the Late Cretaceous, prior to the onset of magmatism. However, biostratigraphic control on the timing of Deccan uplift is generally not as good as for Emeishan and North Atlantic Provinces. Permanent uplift is also found along the Western Ghats escarpment, firstly as a result of magmatic underplating and secondly by isostatic adjustment caused by scarp recession and the associated erosion and by deposition across the thinned continental margin.

The North Atlantic Igneous Province provides a clear example of how the sedimentological response to regional transient surface uplift depends critically on palaeogeography. Because the NAIP was emplaced across a mosaic of basement blocks and sedimentary basins of varying age and water depths, surface uplift was recorded by a continuous sedimentary succession in some areas and by an erosionsal unconformity in others. This variability is well seen in the British Paleocene Igneous Province and surrounding regions. In Northern Ireland, a Paleocene continental flood basalt succession overlies Cretaceous limestones with an erosional unconformity. It not possible to obtain an accurate estimate of the amplitude of driving uplift from this region because erosion has occurred, and the timing of uplift can only be inferred by making assumptions about limestone denudation rates, similar to the Emeishan case. In contrast, the amplitude and timing of uplift can be measured in detail from continuous sedimentary successions in the surrounding offshore basins. Importantly, the quality and quantity of these data are high because of extensive hydrocarbon exploration. Probably one of the most important results is that more than half of the total transient regional kilometre-scale uplift grew in much less than 1 m.y., immediately before the Paleocene/Eocene Thermal Maximum global climate change event. Another interesting observation is that the NAIP was not associated with growth and decay of a single domal swell. Instead, surface uplift occurred in several discrete events, with Phase 1 magmatism associated with minor uplift localised around igneous centres, and Phase 2 magmatism associated with widespread, kilometre-scale uplift. In principle, such detailed uplift histories might be extracted from other provinces. For example, subsidence anomalies indica-tive of transient uplift similar to those seen in the North Atlantic have been noted in several offshore sedimen-tary basins adjacent to the Deccan Province (Halkett et al., 2001; Halkett, 2002), but the quantity and quality of the published data mean that it is not yet possible to confirm whether or not the uplift occurred on the same rapid timescales and spatial patterns. These examples highlight the importance of studying adjacent continu-ous sedimentary successions in addition to examining erosional contacts at the bases of continental flood basalt successions.

Several lines of evidence indicate that a mantle plume can explain the volcanic, faulting, and uplift histories associated with the 700-km long, 16 m.y. track of the Yellowstone igneous system. Features include: (1) uplift documented to occur in advance (northeast) of the progression of rhyolitic, caldera-forming volcanism; (2)

the Yellowstone Crescent of High Terrain is several hundred kilometres across; (3) northeastward progression of volcanism; (4) the change of type and distribution of volcanism, from the widespread activity at about 16 Ma in the oldest part of the Snake River Plain–Yellowstone volcanic province (plume head), to the spatially restricted volcanism in the eastern Snake River Plain at ∼ 10 Ma, to the present linear 50- to 90-km-wide track (plume tail); (5) the 10- to 2-Ma volcanic track which is coincident in both direction and rate with North American plate motion; (6) the patterns of bands of faulting that extend south and west from Yellowstone (Pierce and Morgan, 1992); and (7) the highest rates of faulting are seen to migrate northeastwards with the onset of hotspot magmatism (Anders, 1994). The mechanism of uplift associated with a thermal plume head or tail does provide a driving process below the lithosphere to explain epeirogenic-type uplift. Palaeo-botanical studies suggest the Basin and Range of Nevada was as much as one kilometre higher than present (Wolfe et al., 1997) in mid-Miocene time in the inferred plume head area (Fig. 9; Pierce et al., 2002). Elsewhere, Molnar and England (1990a) examined the geophysical basis of uplift and question evidence suggesting true uplift as distinct from isostatic uplift associated with erosion. Other researchers considering the origin of the Snake River Plain–Yellowstone Plateau volcanic province have invoked non-plume models. These are discussed by Pierce and Morgan (1992) and Pierce et al. (2002), who conclude that none of these models take into account all of the features which must be considered. Most of the Yellowstone hotspot track is associated with uplift above a plume tail, although the widespread onset of magmatism around 16 Ma can be directly compared with the uplift observations from the other four igneous provinces described in this paper, and involving uplift above an exanding plume head (Camp and Ross, 2004; Hooper et al., in press).

8.2. Problems with non-plume models

In this section, we highlight examples in which alternatives to a starting plume head model introduced in Section 2.2 fail to explain observations of surface uplift. In the hotcell model, an upper mantle convection cell develops by incubation to give hotter mantle beneath a craton (Anderson et al., 1992; King and Anderson, 1998). Incubation occurs too slowly to explain growth of hundreds of metres of surface uplift within much less than a few million years observed in the North Atlantic and Emeishan provinces. In the North Atlantic Province, kilometre-scale uplift occurred hundreds of kilometres

distant from the Greenland craton, where the hotcell model predicts the downwelling limb of the convection cell should exist (King and Anderson, 1998).

Edge-driven convection models predict that uplift should occur in a linear zone parallel to the lithospheric step that drives the convection. A potential present-day example of edge-driven convection occurs around the margins of southern Africa (King and Ritsema, 2000). There, a linear belt of high topography a few hundred km wide (associated with the Great Escarpment) parallels the lithospheric edge, a corresponding positive long-wavelength free-air gravity anomaly implies dynamic support, and seismic tomographic images can be interpreted in terms of a small-scale convective cell related to the continent/ocean boundary. There is no modern LIP in southern Africa. Moreover, denudational models, and associated thermochronometric data have been usefully employed to explain the escarpment topographies of southern Africa (Gilchrist and Summerfield, 1990; Brown et al., 2000). In contrast, transient surface uplift associated with both the North Atlantic and Deccan provinces was well over 1000 km in radius. In the North Atlantic, significant surface uplift occurred around the British Isles, about 1000 km from the Europe/Greenland break-up zone and the margin of the Greenland craton. In the Deccan province, surface uplift occurred onshore and also offshore both west and east of India, and was clearly not specifically associated with craton or continent/ocean boundaries.

The North Atlantic and Deccan Provinces are both related to continental break-up. It has been suggested that volcanic passive margins such as those observed in both provinces can be generated by rifting above normal temperature mantle, i.e. without a plume head (Mutter et al., 1988; van Wijk et al., 2001). In these models, the active upwelling required to increase melting is driven by small-scale edge-driven convection cells within a narrow rift, enhanced by melt extraction buoyancy. In the North Atlantic, these models cannot explain the British Province, which is situated hundreds of kilometres from the Europe/Greenland break-up zone and was active several m.y. prior onset of rifting leading to break-up, nor the West Greenland Province, which is adjacent to a non-volcanic passive margin (Nielsen et al., 2002). These models cannot easily explain continuing hotspot activity at Iceland today, either (Meyer et al., in press). In the Deccan province, continental separation and associated seafloor spreading occurred after the main igneous activity. Moreover, neither can such small-scale convection models explain widespread transient uplift up to about 1000 km inboard of the continental margins observed in both the North Atlantic and Deccan Provinces.

In the North Atlantic, continental separation and Phase 2 igneous activity were roughly contemporaneous, but it is not possible to appeal to flexural support of the flanks of the new oceanic rift to explain the widespread uplift because the effective elastic thickness of the lithosphere is too low. For example, the effective elastic thickness of the NW European margin is less than 10 km (Fowler and McKenzie, 1989; Tiley et al., 2003). In general, therefore, it is more likely that any small-scale convection related to continental break-up zone acts in addition to, not instead of, a starting plume head to form volcanic margins, as suggested by Keen and Boutilier (2000).

8.3. Problems with starting plume models

It is very difficult to explain voluminous shallow mantle melting and associated widespread kilometre-scale uplift in the igneous provinces discussed here without invoking high mantle temperatures, and the high temperature mantle must be rapidly emplaced in order to explain the rapid onset of uplift and the high flux rates of magma production. These arguments strongly support some form of starting plume head model. However, published variants on the general starting plume head model fail to account for the details of the uplift observations. The rapid growth of dynamic support in the North Atlantic and Emeishan Provinces argues against large-diameter (~ 1000 km) diapiric plume heads envisioned by Griffiths and Campbell (1991). A mantle viscosity of 10^{19} Pas or less is required to achieve the observed uplift timescales of 1 m.y or less. Such low viscosities have been inferred for the asthenosphere, but the rise speed of a 1000 km diameter diapir should be governed by the viscosity of the deeper mantle, because the asthenosphere is only about 100 km thick. It is likely that most of the mantle has a viscosity in the range 10^{20} to 10^{22} Pas (Forte and Mitrovica, 2001) and, therefore, it is doubtful that a 1000-km-diameter diapir can rise fast enough to explain the observed uplift rates.

Starting plume models that involve upwelling within a narrow conduit and predominantly lateral flow within the asthenosphere can reproduce the short timescales of uplift using more realistic mantle properties. Numerical simulations of starting plumes, using a non-Newtonian rheology appropriate for disclocation creep within the asthenosphere, exhibit mantle flow speeds of up to 10 m/yr (Larsen et al., 1999). This sort of model probably has the best potential to satisfy the observations of rapidly inflating transient swells. However, in the North Atlantic example, where detailed information on the time-dependent behaviour of the uplift swell is

available, the details have yet to be worked out satisfactorily. For example, Sleep (1997), Saunders et al. (1997) and Larsen and Saunders (1998) suggested that a single starting plume welled up in the vicinity of Greenland at 61 Ma. Hot mantle spread rapidly within the asthenosphere, so that it lay beneath the entire region from Baffin Island to the British Isles within less than 1 m.y. to generate NAIP Phase 1. The hot layer remained beneath the plate for about 5 m.y. until continental separation, when it was consumed in the production of oceanic lithosphere and generated NAIP Phase 2. This scenario involving a single phase of upwelling is incompatible with the observations of limited regional uplift during the Middle Paleocene and sudden onset of widespread uplift during the Late Paleocene. It is likely that multiple phases of mantle upwelling are required to explain the distinct phases of uplift and igneous activity.

The chemical compositions of many continental flood basalts show that melting occurred to depths as shallow as about 50 km. Lithospheric thinning is required, but there is a long-standing debate over whether thinning is achieved by rifting or by thermo-mechanical erosion of the base of the lithosphere during plume emplacement. One possible solution is that the impingement of the plume on the base of the lithosphere remobilises the lithosphere. Thermal rejuvenation by conduction of heat (Detrick and Crough, 1978; Crough, 1978) is unlikely to explain the cases we discuss here because the transient uplift is to rapid. White and McKenzie (1995) reviewed lithospheric erosion processes (including mechanical erosion and convective instabilities: e.g., Spohn and Schubert, 1982; Liu and Chase, 1989), and concluded that whilst emplacement of a plume head can rapidly remove the lower thermal boundary layer component of the lithosphere, the upper mechanical boundary layer (perhaps the upper 75% of the plate) can only be thinned slowly as heat is conducted into it.

Tanton and Hager (2000), Şengör (2001) and Elkins-Tanton (2005) have emphasised the importance of lithosphere/asthenosphere density and viscosity contrasts in order to explain removal of the mechanically strong lithosphere by gravitational instability. Emplacement of hot, low-density mantle on the base of the lithosphere may trigger downward flow of the overlying higher density lithosphere, and its rapid replacement by plume mantle (Şengör, 2001; Elkins-Tanton, 2005). However, in order to develop the necessary density contrast for delamination to occur, it is likely that the lithosphere (or crust) needs to be partially replaced with dense eclogite (Tanton and Hager, 2000). Solidification of melt to form eclogite would also supply heat to the

mechanically strong lithosphere, thereby reducing its viscosity and further promoting delamination. In this scenario, the key factor is probably whether sufficient melt can pond at mid-lithospheric depths to form eclogite.

In the models of Burov and Guillou-Frottier (2005), delamination occurs without recourse to replacement of lithosphere with eclogite because of coupling between the lithosphere and the plume head. However, there is a lack of evidence for the spatially complex patterns of uplift that are also predicted by this model suggests that this mechanism of delamination is unlikely to occur naturally.

The most obvious way that geological observations can be used directly to decide between rifting and plume-related erosion or delamination is by constraining the degree of rifting associated with each LIP. The rifting history for the previous hundred m.y. is also required in order to establish the contemporary thickness of the mechanical boundary layer by thermal modelling.

Of the five provinces discussed herein, the best information on the previous rifting history is available in the British Paleocene Igneous Province, part of Phase 1 of the North Atlantic Province. Rare earth element distributions show that the top of the melting region was about 70 km (Brodie and White, 1994, 1995; White and McKenzie, 1995) but there was no significant rifting coeval with British Province emplacement, so thinning must have been achieved by lithospheric erosion. The British Province was emplaced within the Sea of the Hebrides Trough, which formed by modest rifting (total strain less than 2) in the Jurssasic (Rowley and White, 1998; Emeleus and Bell, 2005). The adjacent Faroe–Shetland basin underwent greater stretching (total strain more than 2) during the Cretaceous. It is possible that the mechanically strong part of the lithosphere was thinned from a standard thickness of about 100 km to about 70 km during these rifting events, and that the underlying weaker lithosphere was rapidly removed by convective instabilities during emplacement of the hot mantle to form the BPIP (Brodie and White, 1994, 1995).

The Emeishan Province has previously been interpreted to be associated with rifting, but the role of rifting is now debated (He et al., 2003). In the Siberian Province, melting depths as shallow as 40 km must be explained (White and McKenzie, 1995; Reichow et al., 2005). Widespread rifting within the West Siberian Basin with total strain of 1.5–2 (Saunders et al., 2005) might not be sufficient to explain thinning of the mechanically strong lithosphere from about 100 km to 40 km. Localised more intense rifting (total strain 3–4) is inferred from a deep seismic profile but the age of this rifting is not directly constrained (Pavlenkova et al.,

2002; Saunders et al., 2005). Hence the weak lithospheric thermal boundary layer must have been completely removed during emplacement of a plume head, and it is possibly the case that part of the mechanical boundary layer was also weakened and removed, as envisaged by Tanton and Hager (2000), and Elkins-Tanton (2005).

It is interesting to speculate that the location of continental LIPs (generally close to cratons) is not a function of edge-driven convection (e.g., King and Anderson, 1998), but rather is a function of the interplay between hot plume mantle and the density of the overlying lithosphere. Cratonic, low-density mantle lithosphere could retain its buoyancy even above a plume, whereas younger lithosphere, associated with ancient mobile belts or accretionary terranes, may have a denser mantle root which is inherently less stable and more likely to delaminate into the underlying plume. Delamination above a plume may also serve to explain rapid transient pulses of uplift and subsidence over and above the effects of plume emplacement (Şengör, 2001; Elkins-Tanton, 2005).

9. Conclusions

1. All of the five magmatic provinces presented in this paper exhibit surface uplift. In the cases of Deccan, North Atlantic and Emeishan the uplift had both transient and permanent components. For Yellowstone, both the earlier flood basalt province and the later hotspot track are associated with transient surface uplift.

2. Widespread transient surface uplift associated with LIP emplacement is best interpreted as dynamic support in response to mantle convection. Interpretation of permanent isostatic surface uplift related to LIP magmatism is more difficult to interpret directly in terms of mantle convection, unless the mantle source composition, melting and melt transport processes can be constrained.

3. Onset of regional surface uplift preceded magmatism in all five provinces. Biostratigraphic resolution in the sediments that record uplift is best in the North Atlantic and Emeishan Provinces, where onset of significant uplift occurred less than 1 and 2.5 m.y., respectively, before onset of magmatism.

4. The geological record of regional surface uplift depends on pre-uplift palaeogeography, and is also related to pre-existing lithospheric thickness, as well as to the spatial and temporal pattern of uplift. Whilst the LIPs presented here are all associated with regional surface uplift, details of how this signal is

preserved in the erosional or depositional records are unique to each LIP.

5. Rapid onset of widespread transient surface uplift is not easily explained by 'top-down' mantle convection models involving hotcell incubation beneath cratons and/or small-scale convection cells adjacent to steps in the base of the lithosphere.

6. Whilst the general concept of anomalously hot mantle upwelling in a starting plume head can best account for rapid onset of transient regional uplift, published variants on the staring plume model do not explain details of the observations. It is unlikely that the starting plume models advocated by Campbell and Griffiths (1990) and others, and which involve large, diapiric plume heads, can account for the short timescales of uplift. It is more likely that rapid upwelling of hot mantle in narrow jets followed rapid lateral spreading in the asthenosphere can account for observed rapid uplift. Observations of surface uplift do not constrain the depth of origin of these plume heads.

7. The large volumes of tholeiitic continental flood basalts derived by melting at shallow depths requires lithospheric thinning. It is likely that this thinning is achieved by some form of lithospheric erosion in addition to rifting, although the constraints on rifting are not good in many cases. Lithospheric erosion alone cannot explain LIPs, rather it enhances melting during emplacement of a plume head.

8. Further integrated sedimentological, tectonic and petrologic investigation of these provinces is warranted in order to generate high-resolution data of uplift and subsidence; there is still a dearth of detailed field data.

Acknowledgements

References

Adatte, T., Keller, G., Stinnesbeck, W., 2002. Late Cretaceous to early Palaeocene climate and sea-level fluctuations: the Tunisian record. Palaeogeography, Palaeoclimatology, Palaeoecology 178, 165–196.

Al-Kindi, S., White, N., Sinha, M., England, R., Tiley, R., 2003. Crustal trace of a hot convective sheet. Geology 31, 207–210.

Anders, M.H., 1994. Constraints on North American plate velocity from Yellowstone hotspot deformation field. Nature 369, 53–55.

Anders, M.H., Geissman, J.W., Piety, L.A., Sullivan, J.T., 1989. Parabolic distribution of circum-eastern Snake River Plain seismicity and latest Quaternary faulting: migratory pattern and association with the Yellowstone hotspot. Journal of Geophysical Research 94, 1589–1621.

Anderson, D.L., 1994. The sub lithospheric mantle as the source of continental flood basalts; the case against the continental lithosphere and plume head reservoirs. Earth and Planetary Science Letters 123, 269–280.

Anderson, D.L., 2000. The thermal state of the upper mantle; no role for mantle plumes. Geophysical Research Letters 27, 3623–3626.

Anderson, D.L., 2001. Top-down tectonics? Science 293, 2016–2018.

Anderson, R.N., McKenzie, D.P., Sclater, J.G., 1973. Gravity, bathymetry and convection within the Earth. Earth and Planetary Science Letters 18, 391–407.

Anderson, D.L., Zhang, Y.-S., Tanimoto, T., 1992. Plume heads, continental lithosphere, flood basalts and tomography. In: Storey, B.C., Alabaster, T., Pankhurst, R.J. (Eds.), Magmatism and the Causes of Continental Break-up. Geological Society of London Special Publication, vol. 68. Geological Society of London, pp. 99–124.

Armstrong, R.L., Leeman, W.P., Malde, H.E., 1975. K–Ar dating, Quaternary and Neogene rocks of the Snake River Plain, Idaho. American Journal of Science 275, 225–251.

Artemieva, I.M., Mooney, W.D., 2001. Thermal thickness and evolution of Precambrian lithosphere: a global study. Journal of Geophysical Research 106 (B8), 16387–16414.

Baksi, A.K., 1990. Timing and duration of Mesozoic–Tertiary flood-basalt volcanism. Eos, Transactions of the American Geophysical Union 71, 1835–1836.

Baksi, A.K., 1994. Geochronological studies on whole-rock basalts, Deccan Traps, India — evaluation of the timing of volcanism relative to the K–T boundary. Earth and Planetary Science Letters 121, 43–56.

Baksi, A.K., Ferrar, E., 1991. Ar/Ar dating of the Siberian Traps, USSR: evaluation of the ages of the two main extinction events relative to episodes of flood basalt volcanism in the USSR and Deccan Traps, India. Geology 19, 461–464.

Barton, A.J., White, R.S., 1997. Crustal structure of Edoras Bank continental margin and mantle thermal anomalies beneath the North Atlantic. Journal of Geophysical Research 102, 3109–3129.

Basu, A.R., Renne, P.R., Dasgupta, D.K., Teichmann, F., Poreda, R.J., 1993. Early and late alkali igneous pulses and a high-^{3}He plume origin for the Deccan flood basalts. Science 261, 902–906.

Biswas, S.K., 1987. Regional tectonic framework, structure and evolution of the western marginal basins of India. Tectonophysics 135, 307–327.

Bown, J.W., White, R.S., 1995. Effect of finite extension rate on melt generation at rifted continental margins. Journal of Geophysical Research 100, 18011–18029.

Brodie, J., White, N., 1994. Sedimentary basin inversion caused by igneous underplating: Northwest European continental shelf. Geology 22, 147–150.

Brodie, J., White, N., 1995. The link between sedimentary basin inversion and igneous underplating. In: Buchanan, J., Buchanan, P.

(Eds.), Basin Inversion. Geological Society, London, Special Publication, vol. 88, pp. 21–38.

Brown, R., Gallagher, K., Gleadow, A.J., Summerfield, M.A., 2000. Morphotectonic evolution of the South Atlantic margins of Africa and South America. In: Summerfield, M.A. (Ed.), Geomorphology and Global tectonics. Wiley, pp. 255–281.

Bunge, H.-P., Richards, M.A., Baumgartner, J.R., 1997. A sensitivity study of three-dimensional mantle convection at 108 Rayleigh number: effects of depth dependent viscosity, heating mode, and an endothermic phase change. Journal of Geophysical Research 102, 11991–12007.

Burke, K., Dewey, J.F., 1973. Plume generated triple junctions: key indicators in applying plate tectonics to old rocks. Journal of Geology 81, 406–433.

Burke, K., Wilson, J.T., 1972. Is the African Plate stationary? Nature 239, 387–390.

Burov, E., Guillou-Frottier, L., 2005. The plume head-continental lithosphere interaction using a tectonically realistic formulation for the lithosphere. Geophysical Journal International 161, 469–490.

Camp, V.E., 1995. Mid-Miocene propagation of the Yellowstone mantle plume head beneath the Columbia River Basalt source region. Geology 23, 435–438.

Camp, V.E., Ross, M.E., 2004. Mantle dynamics and genesis of mafic magmatism in the intermontane Pacific Northwest. Journal of Geophysical Research 109 (B08204) 14 pp.

Campbell, I.H., Griffiths, R.W., 1990. Implication of mantle plume structure for the evolution of flood basalts. Earth and Planetary Science Letters 99, 79–93.

Campbell, I.A., Czamanske, G.K., Fedorenko, V.A., Hill, R.I., Stepanov, V., 1992. Synchronism of the Siberian Traps and the Permian–Triassic boundary. Science 258, 1760–1763.

Carson, R.W., Hart, W.K., 1988. Flood basalt volcanism in the northwestern United States. In: Macdougall, J.D. (Ed.), Continental Flood Basalts. Kluwer Academic Publishers, Dordrecht, The Netherlands, pp. 35–61.

Ceramicola, S., Stoker, M., Praeg, D., Shannon, P.M., De Santis, L., Hoult, R., Hjelstuen, B.O., Laberg, S., Mathiesen, A., 2005. Anomalous Cenozoic subsidence along the 'passive' continental margin from Ireland to mid-Norway. Marine and Petroleum Geology 22, 1045–1067.

Chaubey, A.K., Bhattacharya, G.C., Murty, G.P.S., Srinivas, K., Ramprasad, T., Gopala Rao, D., 1998. Early Tertiary seafloor spreading magnetic anomalies and paleo-propagators in the northern Arabian Sea. Earth and Planetary Science Letters 154, 41–52.

Christiansen, R.L., 2001. The Quaternary and Pliocene Yellowstone Plateau volcanic field of Wyoming, Idaho, and Montana. U.S. Geological Survey Professional Paper 729 G. 145 pp.

Christiansen, R.L., Yeats, R.S., 1992. Post-Laramide geology of the U.S. Cordilleran region. In: Burchfiel, B.C., Lipman, P.W., Zoback, M.L. (Eds.), The Cordilleran Orogen: Conterminous U.S. Geology of North America, G-3. Geological Society of America, Boulder, Colorado, pp. 261–406.

Christiansen, R.L., Foulger, G.R., Evans, J.R., 2002. Upper mantle origin of the Yellowstone hotspot. GSA Bulletin 114, 1245–1256.

Chung, S.L., Jahn, B.M., Wu, G.Y., Lo, C.H., Cong, B.L., 1998. The Emeishan flood basalt in SW China: A mantle plume initiation model and its connection with continental break-up and mass extinction at the Permian–Triassic boundary. In: Flower, M., Chung, S.L., Lo, C.H. (Eds.), Mantle dynamics and plate interaction in East Asia. AGU Monograph, vol. 27. American Geophysical Union, Washington, D.C., pp. 47–58.

Clift, P.D., Turner, J., 1998. Paleogene igneous underplating and subsidence anomalies in the Rockall–Faeroe–Shetland area. Marine and Petroleum Geology 15, 223–243.

Clift, P.D., Carter, A., Hurford, A.J., 1998. The erosional and uplift history of NE Atlantic passive margins: constraints on a passing plume. Journal of the Geological Society 155, 787–800.

Coffin, M.F., Eldholm, O., 1994. Large igneous provinces: crustal structure, dimensions, and external consequences. Reviews of Geophysics 32, 1–36.

Collier, J.S., Minshull, T.A., Kendall, J.-M., Whitmarsh, R.B., Rümpker, G., Joseph, P., Samson, P., Lane, C.I., Sansom, V., Vermeesch, P.M., Hammond, J., Wookey, J., Teanby, N., Ryberg, T.M., Dean, S.M., 2004. Rapid Continental Breakup and Microcontinent Formation in the Western Indian Ocean. Eos, Transactions of the American Geophysical Union 85 (46), 481. doi:10.1029/2004EO460001.

Collier, J.S., Hall, F., Sansom, V., Minshull, T.A., Whitmarsh, R.B., Kendall, J.-M., Vardy, M.E., Lane, C.I., 2005. Crustal structure of the rifted northeast of the Seychelles Bank, western Indian Ocean. Geophysical Research Abstracts 7, 08007 (EGU05).

Courtillot, V., Besse, J., Vandamme, D., Montigny, R., Jaeger, J.J., Capetta, H., 1986. Deccan flood basalts at the Cretaceous–Tertiary boundary? Earth and Planetary Science Letters 80, 361–374.

Courtillot, V., Feraud, G., Maluski, H., Vandamme, D., Moreau, M.G., Besse, J., 1988. Deccan flood basalts and the Cretaceous–Tertiary boundary. Nature 333, 843–846.

Courtillot, V.E., Jaupart, C., Manighetti, I., Tapponnier, P., Besse, J., 1999. On causal links between flood basalts and continental break-up. Earth and Planetary Science Letters 166, 177–195.

Courtney, R., White, R., 1986. Anomalous heat flow and geoid across the Cape Verde Rise: evidence for dynamic support from a thermal plume in the mantle. Geophysical Journal of the Royal Astronomical Society 87, 815–867.

Cox, K.G., 1980. A model for flood basalt volcanism. Journal of Petrology 21, 629–650.

Cox, K.G., 1989. The role of mantle plumes in the development of continental drainage patterns. Nature 342, 873–877.

Cox, K.G., 1993. Continental magmatic underplating. Philosophical Transactions of the Royal Society. A 342, 155–166.

Cox, K.G., Hawkesworth, C.J., 1984. Relative contribution of crust and mantle to flood basalt volcanism, Mahabaleshwar area, Deccan Traps. Philosophical Transactions of the Royal Society of London 310, 627–641.

Cripps, J.A., 2002. Environmental impact of Deccan Trap flood basalt volcanism: assessment of regional floral responses to late Cretaceous – early Tertiary activity. PhD Thesis, The Open University, Milton Keynes, UK.

Cripps, J.A., Widdowson, M., Spicer, R.A., Jolley, D.W., 2005. Coastal ecosystem responses to late-stage Deccan Trap volcanism: the post K–T boundary (Danian) palynofacies of Mumbai (Bombay), west India. Palaeogeography, Palaeoclimatology, Palaeoecology 216, 303–332.

Crough, S.T., 1978. Thermal origin of mid-plate hotspot swells. Geophysical Journal of the Royal Astronomical Society 55, 451–469.

Czamanske, G.K., Gurevitch, V., Fedorenko, V., Simonov, O., 1998. Demise of the Siberian plume: palaeogeographic and palaeotectonic reconstruction from the pre-volcanic and volcanic record, north-central Siberia. International Geology Review 40, 95–115.

Dam, G., Larsen, M., Sønderholm, M., 1998. Sedimentary response to mantle plumes: implications from Paleocene onshore reconstructions, West and East Greenland. Geology 26, 207–210.

Davies, G.F., 1994. Thermomechanical Erosion of the Lithosphere by Mantle Plumes. Journal of Geophysical Research, [Solid Earth] 99 (B8), 15709–15722.

Davies, J.H., Bunge, H.P., 2006. Are splash plumes the origin of minor hotspots? Geology 34, 349–352.

Deptuck, M.E., MacRae, R.A., Shimeld, J.W., Williams, G.L., Fensome, R.A., 2003. Revised Upper Cretaceous and lower Paleogene lithostratigraphy and depositional history of the Jeanne d'Arc Basin, offshore Newfoundland, Canada. American Association of Petroleum Geologists Bulletin 87, 1459–1483.

Detrick, R.S., Crough, S.T., 1978. Island subsidence, hotspots, and lithosphere thinning. Journal of Geophysical Research 83, 1236–1244.

Devey, C.W., Lightfoot, P.C., 1986. Volcanology and tectonic control of stratigraphy and structure in the western Deccan Traps. Bulletin of Volcanology 48, 195–207.

Devey, C.W., Stephens, W.E., 1991. Tholeiitic dykes in the Seychelles and the original spatial extent of the Deccan. Journal of the Geological Society (London) 148, 979–983.

Draper, D.S., 1991. Late Cenozoic bimodal magmatism in the northern Basin and Range Province of Southeastern Oregon. Journal of Volcanology and Geothermal Research 47, 299–328.

Duncan, R.A., Hargreaves, R.B., 1990. $^{40}Ar/^{39}Ar$ geochronology of basement rocks from the Mascarene plateau, the Chagos Bank, and the Maldives Ridge. Proc. ODP, Sci. Results, vol. 115, pp. 43–51.

Duncan, R.A., Pyle, D.G., 1988. Rapid eruption of the Deccan flood basalts at the Cretaceous–Tertiary boundary. Nature 333, 841–843.

Ebdon, C.C., Granger, P.J., Johnson, H.D., Evans, A.M., 1995. Early Tertiary evolution and sequence stratigraphy of the Faroe–Shetland Basin: implications for hydrocarbon prospectivity. In: Scrutton, R.A., Stoker, M.S., Shimmield, G.B., Tudhope, A.W. (Eds.), The Tectonics, Sedimentation and Palaeoceanography of the North Atlantic Region. Geological Society of London Special Publication, vol. 90. Geological Society of London, pp. 51–69.

ECS (Editing Committee of Stratigraphy), 2000. Permian in China. Geological Publishing House, Beijing. 149 pp.

Elkins-Tanton, L.T., 2005. Continental magmatism caused by lithospheric delamination. In: Foulger, G.R., Natland, J.H., Presnall, D.C., Anderson, D.L. (Eds.), Plates, Plumes and Paradigms. Special Paper, vol. 388. Geological Society of America, Boulder, Colorado, pp. 449–461.

Emeleus, C.H., Bell, B.R., 2005. The Palaeogene Volcanic Districts of Scotland. British Geological Survey. 214 pp.

Ernst, R.E., Buchan, K.L., 2003. Recognizing Mantle Plumes in the geological record. Annual Review of Earth and Planetary Sciences 31, 469–523.

Farnetani, C.G., Richards, M.A., 1994. Numerical investigation of the mantle plume initiation model for flood basalt events. Journal of Geophysical Research 99, 13813–13833.

Fedorenko, V.A., Lightfoot, P.C., Naldrett, A.J., Czamanske, G.K., Hawkesworth, C.J., Wooden, J.L., Ebel, D.S., 1996. Petrogenesis of the Siberian flood-basalt sequence at Noril'sk, north central Siberia. International Geology Review 38, 99–135.

Feng, Z.Z., Yang, Y.Q., Jin, Z.K., 1997. Lithofacies paleography of Permian of south China. Petroleum University Press, Beijing. 242 pp. (in Chinese with English abstract).

Forte, A.M., Mitrovica, J.X., 2001. Deep-mantle high-viscosity flow and thermochemical structure inferred from seismic and geodynamic data. Nature 410, 1049–1056.

Fowler, S.R., McKenzie, D.P., 1989. Gravity studies of the Rockall and Exmouth Plateaux using SEASAT altimetry. Basin Research 2, 27–34.

Gallet, Y., Weeks, R., Vandamme, D., Courtillot, V., 1989. Duration of Deccan Trap volcanism — a statistical approach. Earth and Planetary Science Letters 93, 273–282.

Gilchrist, A.R., Summerfield, M.A., 1990. Differential denudation and the flexural isostasy in the formation of rifted-margin upwarps. Nature 346, 739–742.

Goel, L.R., Mumtaz, S.Z., Gupta, R., Keller, G., Li, L., MacLeod, N., 1996. The Cretaceous–Tertiary boundary stratotype section at El Kef, Tunisia: how catastrophic was the mass extinction? Palaeogeography, Palaeoclimatology, Palaeoecology 119, 221–254.

Gradstein, F.M., Ogg, J.G., Smith, A.G., Bleeker, W., Lourens, L.J., 2004. A new geologic time scale, with special reference to Precambrian and Neogene. Episodes 27, 83–100.

Griffiths, R.W., Campbell, I.H., 1991. Interaction of mantle plume heads with the Earth's surface and onset small-scale convection. Journal of Geophysical Research 96, 18275–18310.

Guillou, L., Jaupart, C., 1995. On the effects of continents on mantle convection. Journal of Geophysical Research 100, 24217–24238.

Gunnell, Y., Gallagher, K., Carter, A., Widdowson, M., Hurford, A.J., 2003. Denudation history of the continental margin of western peninsular India since the early Mesozoic — reconciling apatite fission track data with geomorphology. Earth and Planetary Science Letters 215, 187–201.

Halkett, A., 2002. Mantle plume control on subsidence and sedimentation, onshore-offshore India. Unpublished PhD Thesis, University of Cambridge, Cambridge, UK.

Halkett, A., White, N., Chandra, K., Lal, N.K., 2001. Dynamic uplift of the Indian Peninsula and the Réunion Plume. AGU, Fall Meeting, Abstract T11A-0845.

Hamilton, W.B., 2003. An alternative Earth. GSA Today 13 (11), 4–12.

Hanski, E., Walker, R.J., Huhma, H., Polyakov, G.V., Balykin, T.T., Hoa, Phuong, N.T., 2004. Origin of the Permian–Triassic komatiites, northwestern Vietnam. Contributions to Mineralogy and Petrology 147, 453–469.

He, B., Xu, Y.G., Chung, S.L., Xiao, L., Wang, Y.M., 2003. Sedimentary evidence for a rapid, kilometer scale crustal doming prior to the eruption of the Emeishan flood basalts. Earth and Planetary Science Letters 213, 391–405.

He, B., Xu, Y.G., Wang, Y.M., Luo, Z.Y., 2006. Sedimentation and lithofacies paleogeography in SW China before and after the Emeishan flood volcanism: new insights into surface response to mantle plume activity. Journal of Geology 114, 117–132.

Hirschmann, M.M., Stolper, E.M., 1996. A possible role for garnet pyroxenite in the origin of the 'garnet signature' in MORB. Contributions to Mineralogy and Petrology 124, 185–208.

Hofmann, C., Féraud, G., Courtillot, V., 2000. $^{40}Ar/^{39}Ar$ dating of mineral separates and whole rocks from the Western Ghats lava pile: further constraints on duration and age of the Deccan traps. Earth and Planetary Science Letters 180, 13–27.

Hooper, P.R., 1990. The timing of crustal extension and the eruption of continental flood basalts. Nature 345, 246–249.

Hooper, P.R., Camp, V.E., Reidel, S.P., Ross, M.E., in press. Origin of the Columbia River Flood Basalts: Plume vs. Nonplume Models. In: Foulger, G.R., Jurdy, D.M. (Eds.), The Origins of Melting Anomalies: Plates, Plumes, and Planetary Processes, Geological Society of America Special Paper (scheduled 2007).

Humphreys, E.D., Dueker, K.G., Schutt, D.L., Smith, R.B., 2000. Beneath Yellowstone: evaluating plume and non-plume models using teleseismic images of the upper Mantle. GSA Today 10, 1–6.

Janecke, S.U., Hammond, B.F., Snee, L.W., Geissman, J.W., 1997. Rapid extension in an Eocene volcanic arc: structure and

stratigraphy of an Eocene–Oligocene supra-detachment basin, Muddy Creek half graben in central Idaho. Geological Society of America Bulletin 109, 253–267.

Jaques, A.L., Green, D.H., 1980. Anhydrous melting of peridotite at 0–15 Kb pressure and the genesis of tholeiitis basalts. Contributions to Mineralogy and Petrology 73, 287–310.

Jaworowski, C., 1994. Geologic implications of Quaternary tephra localities in the western Wind River Basin, Wyoming. In: Keefer, W.R., Metzger, S.J., Godwin, L.H. (Eds.), Oil and Gas and Other Resources of the Wind River Basin, Wyoming: Wyoming Geological Association Special Symposium, pp. 191–205.

Jones, S.M., 2000. Effect of the Iceland Plume on Cenozoic sedimentation patterns. Unpublished Ph.D. dissertation, University of Cambridge, UK.

Jones, R.W., Milton, N.J., 1994. Sequence development during uplift: paleogene stratigraphy and relative sea-level history of the Outer Moray Firth, UK North Sea. Marine and Petroleum Geology 11, 157–165.

Jones, S.M., White, N., 2003. Shape and size of the starting Iceland plume swell. Earth and Planetary Science Letters 216, 271–282.

Jones, S.M., White, N., Lovell, B., 2001. Cenozoic and Cretaceous transient uplift in the Porcupine Basin and its relationship to a mantle plume. Geological Society of London, Special Publication 188, 345–360.

Jones, S.M., White, N., Maclennan, J., 2002. V-shaped ridges around Iceland: implications for spatial and temporal patterns of mantle convection. Geochemistry Geophysics Geosystems 3.

Jordan, B.T., Grunder, A.L., Duncan, R.A., Deino, A.L., 2004. Geochronology of age-progressive volcanism of the Oregon High Lava Plains: implications for the plume interpretation of Yellowstone. Journal of Geophysical Research 109, B10202. doi:10.1029/2003JB002776.

Kamo, S.L., Czamanske, G.K., Amelin, Y., Fedorenko, A., Davis, D.W., Trofimov, V.R., 2003. Rapid eruption of Siberian flood-volcanic rocks and evidence for coincidence with the Permian–Triassic boundary and mass extinction at 251 Ma. Earth and Planetary Science Letters 214, 75–91.

Keen, C.E., Boutilier, R.R., 2000. Interaction of rifting and hot horizontal plume sheets at volcanic margins. Journal of Geophysical Research 105, 13375–13387.

Kennett, B.L.N., Widiyantoro, S., 1999. A low seismic wavespeed anomaly beneath northwestern India: a seismic signature of the Deccan plume? Earth and Planetary Science Letters 165, 145–155.

King, S.D., Anderson, D.L., 1995. An alternative mechanism of flood basalt formation. Earth and Planetary Science Letters 136, 269–279.

King, S.D., Anderson, D.L., 1998. Edge-driven convection. Earth and Planetary Science Letters 160, 289–296.

King, S.D., Ritsema, J., 2000. African hotspot volcanism: small-scale convection in the upper mantle beneath cratons. Science 290, 1137–1140.

Knox, R.W.O.'B., 1998. The tectonic and volcanic history of the North Atlantic region during the Paleocene–Eocene transition: implications for NW European and global biotic events. In: Aubrey, M.-P., Lucas, S.G., Berggren, W.A. (Eds.), Late Paleocene-Early Eocene Climatic and Biotic Events in the Marine and Terrestrial Records. Columbia University Press, pp. 91–102.

Korenaga, J., 2004. Mantle mixing and continental break-up magmatism. Earth and Planetary Science Letters 218, 463–473.

Larsen, H.C., Saunders, A.D., 1998. Tectonism and volcanism at the southeast Greenland rifted margin: a record of plume impact and later continental rupture. In: Saunders, A.D., Larsen, H.C., Clift, P.D., Wise, S.W. (Eds.), Proceedings of the Ocean Drilling Program Scientific Results, vol. 152, pp. 503–533.

Larsen, T.B., Yuen, D.A., Storey, M., 1999. Ultrafast mantle plumes and implications for flood basalt volcanism in the North Atlantic region. Tectonophysics 311, 31–43.

Li, L., Keller, G., Adatte, T., Stinnesbeck, W., 2000. Late Cretaceous sea-level changes in Tunisia: a multidisciplinary approach. Journal of the Geological Society (London) 157, 447–458.

Lightfoot, P.C., Hawkesworth, C.J., Sethna, S.F., 1987. Petrogenesis of rhyolites and trachytes from the Deccan Trap — Sr, Nd and Pb isotope and trace element evidence. Contributions to Mineralogy and Petrology 95, 44–54.

Liu, J.H., Liu, F.T., He, J.K., Chen, H., You, Q.Y., 2001. Study of seismic tomography in Panxi paleorift area of southwestern China — structural features of crust and mantle and their evolution. Science in China, Series D 44, 277–288.

Liu, M., Chase, C.G., 1989. Evolution of midplate hotspot swells: numerical solutions. Journal of Geophysical Research 94, 5571–5584.

Liu, X., Galloway, W.E., 1997. Quantitative determination of tertiary sediment supply to the North Sea Basin. Bulletin American Association of Petroleum Geologists 81, 1482–1509.

Lowry, A.R., Ribe, N.M., Smith, R.B., 2000. Dynamic elevation of the Cordillera, western United States. Journal of Geophysical Research 105, 23371–23390.

Mackay, L.M., Turner, J., Jones, S.M., White, N.J., 2005. Cenozoic vertical motions in the Moray Firth Basin associated with initiation of the Iceland Plume. Tectonics 24 (Art. No. TC5004 SEP 22 2005).

Maclennan, J.C., Jones, S.M., 2006. Regional uplift, gas hydrate dissociation and the origins of the Paleocene/Eocene thermal maximum. Earth and Planetary Science Letters 245, 65–80.

Maclennan, J., Lovell, B., 2002. Control of regional sea-level by surface uplift and subsidence caused by magmatic underplating of Earth's crust. Geology 30, 675–678.

Maggi, A., Jackson, J.A., McKenzie, D., Priestley, K., 2000. Earthquake focal depths, effective elastic thickness, and the strength of the continental lithosphere. Geology 28, 495–498.

McKenzie, D.P., 1978. Some remarks on the development of sedimentary basins. Earth and Planetary Science Letters 40, 25–32.

McKenzie, D., 2003. Estimating T–e in the presence of internal loads. Journal of Geophysical Research 108 (Art. No. 2438 SEP 19 2003).

McKenzie, D., Bickle, M.J., 1988. The volume and composition of melt generated by extension of the lithosphere. Journal of Petrology 29, 625–679.

McKenzie, D., Fairhead, D., 1997. Estimates of the effective elastic thickness of the continental lithosphere from Bouguer and free-air gravity anomalies. Journal of Geophysical Research 102, 27523–27552.

McMillan, M.E., Heller, P.L., Wing, S.L., 2006. History and causes of post-Laramide relief in the Rocky Mountain orogenic plateau. Geological Society of America Bulletin 118 (3–4), 393–405.

McNutt, M.K., Judge, A.V., 1990. The superswell and mantle dynamics beneath the South-Pacific. Science 248, 969–975.

Meyer, R., van Wijk, J., Gernigon, L., in press. North Atlantic Igneous Province: A review of models for its formation. In: Foulger, G.R., Jurdy, D.M. (Eds), Plates, Plumes, and Planetary Processes. Geological Society of America Special Paper 430.

Milanovskiy, Y.Y., 1976. Rift zones of the geologic past and their associated formations. International Geology Review 18, 619–639.

Milbert, D.G., 1991. GEOID90: a high-resolution geoid for the United States. Eos, Transactions of the American Geophysical Union 72, 545–554.

Milton, N.J., Bertram, G.T., Vann, I.R., 1990. Early Palaeogene tectonics and sedimentation in the Central North Sea. In: Hardman,

R.F.P., Brooks, J. (Eds.), Tectonic Events Responsible for Britain's Oil and Gas Reserves. Geological Society, London, Special Publication, vol. 55, pp. 339–351.

Mitchell, C., Widdowson, M., 1991. A geological map of the Southern Deccan Traps, India and its structural implications. Journal of the Geological Society (London) 148, 495–505.

Mohabey, D.M., Samant, B., 2005. Lacustrine facies associated of a Maastrichtian lake (Lameta Formation) from Deccan volcanic terrain Central India: implications to depositional history, sediment cyclicity and climates. Gondwana Geological Magazine, Special Publication 8, 37–52.

Mohabey, D.M., Udhoji, S.G., Verma, K.K., 1993. Palaeontological and sedimentological observations on non-marine Lameta Formation (Upper Cretaceous) of Maharashtra, India: their palaeontological and palaeoenvironmental significance. Palaeogeography, Palaeoclimatology, Palaeoecology 105, 83–94.

Molnar, P., England, P., 1990a. Surface uplift, uplift of rocks, and exhumation of rocks. Geology 18, 1173–1177.

Molnar, P., England, P., 1990b. Late Cenozoic uplift of mountain ranges and global climate change: chicken or egg? Nature 346, 29–34.

Morgan, W.J., 1971. Convection plumes in the lower mantle. Nature 230, 42–43.

Morgan, W.J., 1972. Plate motions and deep mantle convection. Geological Society of America, Memoir 132, 7–22.

Morgan, J.P., Morgan, W.J., Price, E., 1995. Hotspot melting generates both hotspot volcanism and a hotspot swell? Journal of Geophysical Research 100, 8045–8062.

Morgan, L.A., Pierce, K.L., McIntosh, W.C., 2005. Patterns of rhyolitic volcanism along the track of the Yellowstone hotspot. Geochimica et Cosmochimica Acta 69, A142.

Mudge, D.C., Jones, S.M., 2004. Palaeocene uplift and subsidence events in the Scotland–Shetland and North Sea region and their relationship to the Iceland Plume. Journal of the Geological Society (London) 161, 381–386.

Mutter, J.C., Buck, W.R., Zehnder, C.M., 1988. Convective partial melting. 1. A model for the formation of thick basaltic sequences during the initiation of spreading. Journal of Geophysical Research, B 93, 1031–1048.

Nadin, P.A., Kusznir, N.J., Cheadle, M.J., 1997. Early Tertiary plume uplift of the North Sea and Faeroe–Shetland Basins. Earth and Planetary Science Letters 148, 109–127.

Nielsen, T.K., Larsen, H.C., Hopper, J.R., 2002. Contrasting rifted margin styles south of Greenland: implications for mantle plume dynamics. Earth and Planetary Science Letters 200, 271–286.

Nikishin, A.M., Ziegler, P.A., Abbott, D., Brunet, M.-F., Cloetingh, S., 2002. Permo–Triassic intraplate magmatism and rifting in Eurasia: implications for mantle plumes and mantle dynamics. Tectonophysics 351, 3–39.

Parsons, B., Daly, S., 1983. The relationship between surface-topography, gravity-anomalies, and temperature structure of convection. Journal of Geophysical Research 88, 1129–1144.

Pattanayak, S.K., Shrivastava, J.P., 1999. Petrography and major-oxide geochemistry of basalts from the Eastern Deccan Volcanic Province, India. Memoirs of the Geological Society of India 43, 233–270.

Pavlenkova, G.A., Priestley, K., Cipar, J., 2002. 2D model of the crust and uppermost mantle along rift profile, Siberian craton. Tectonophysics 355, 171–186.

Peterson, J.A., Clarke, J.W., 1991. Geology and Hydrocarbon Habitat of the West Siberian Basin. AAPG Studies in Geology, vol. 32.

American Association of Petroleum Geologists, Tulsa, Oklahoma. 93 pp.

Pierce, K.L., Morgan, L.A., 1990. The track of the Yellowstone hotspot: Volcanism, faulting, and uplift. U.S. Geological Survey Open-File Report, vol. 90–413. 85 pp.

Pierce, K.L., Morgan, L.A., 1992. The track of the Yellowstone hotspot: volcanism, faulting, and uplift. In: Link, P.K., Kuntz, M.A., Platt, L.B. (Eds.), Regional Geology of Eastern Idaho and Western Wyoming. Geological Society of America Memoir, vol. 179, pp. 1–53.

Pierce, K.L., Morgan, L.A., 2005. Asymmetrical features across the Yellowstone hotspot track and the northwest inclination of the Yellowstone plume. Geological Society of America Abstracts with Programs 37, 127.

Pierce, K.L., Morgan, L.A., Saltus, R.W., 2002. Yellowstone plume head: postulated tectonic relations to the Vancouver slab, continental boundaries, and climate. In: Bonnichsen, W., White, C.M., McCurry, M. (Eds.), Tectonic and Magmatic Evolution of the Snake River Plain Volcanic Province. Idaho Geological Survey Bulletin, vol. 30, pp. 5–34.

Prasad, G.V.R., Khajuria, C.K., 1995. Implications of the infra- and inter-trappean biota from the Deccan, India, for the role of volcanism in Cretaceous–Tertiary boundary extinctions. Journal of the Geological Society (London) 152, 289–296.

Reddy, P.R., Koteswara Rao, P., Sain, K., 1999. Crustal configuration of the Narmada–Son lineament in Central India from deep seismic sounding studies. Memoirs of the Geological Society of India 43 (1), 353–366.

Reichow, M.K., Saunders, A.D., White, R.V., Pringle, M.S., Al'Mukhamedov, A.I., Medvedev, A.L., Korda, N., 2002. New ^{40}Ar–^{39}Ar data on basalts from the West Siberian Basin: extent of the Siberian flood basalt province doubled. Science 296, 1846–1849.

Reichow, M.K., Saunders, A.D., White, R.V., Al'Mukhamedov, A.I., Medvedev, A.L., 2005. Geochemistry and petrogenesis of basalts from the West Siberian Basin: an extension of the Siberian Traps, Russia. Lithos 79, 425–452.

Ren, S.C., Skogseid, J., Eldholm, O., 1998. Late Cretaceous–Paleocene extension on the Vøring volcanic margin. Marine Geophysical Researches 20, 343–369.

Reynolds, R., 1994. Quantitative analysis of submarine fans in the Tertiary of the North Sea Basin. Marine and Petroleum Geology 11, 202–207.

Ribe, N.M., Christensen, U.R., 1994. Three-dimensional modeling of plume–lithosphere interaction. Journal of Geophysical Research 99, 669–682.

Richards, M.A., Duncan, R.A., Courtillot, V.E., 1989. Flood basalts and hotspot tracks: plume heads and tails. Science 246, 103–107.

Rowley, E., White, N., 1998. Inverse modelling of extension and denudation in the East Irish Sea and surrounding areas. Earth and Planetary Science Letters 161, 57–71.

Salil, M.S., Shrivastava, J.P., 1996. Trace and REE signatures in the Maastrichtian Lameta beds for the initiation of Deccan volcanism before KTB. Current Science 70, 399–401.

Salil, M.S., Shrivastava, J.P., Pattanayak, S.K., 1997. Similarities in the mineralogical and geochemical attributes of detrital clays of Maastrichtian Lameta Beds and weathered Deccan basalt, Central India. Chemical Geology 136, 25–32.

Samant, B., Mohabey, D.M., 2005. Response of flora to Deccan volcanism: a case study from Nand–Dongargaon basin of Maharashtra, implications to environment and climate. Gondwana Geological Magazine 8, 151–164.

Saunders, A.D., Fitton, J.G., Kerr, A.C., Norry, M.J., Kent, R.W., 1997. The North Atlantic Igneous Province. In: Mahoney, J.J., Coffin, M.F. (Eds.), Large Igneous Provinces: Continental, Oceanic and Planetary. Geophysical Monograph, vol. 100. American Geophysical Union, Washington, DC, pp. 45–93.

Saunders, A.D., England, R.W., Reichow, M.K., White, R.V., 2005. A mantle plume origin for the Siberian Traps: uplift and extension in the West Siberian Basin, Russia. Lithos 79, 407–424.

Şengör, A.M.C., 2001. Elevation as indicator of mantle-plume activity. In: Ernst, R.E., Buchan, K.L. (Eds.), Mantle Plumes: Their Identification Through Time. Geological Society of America Special Paper, vol. 352, pp. 183–225.

Sethna, S.F., 1999. Geology of Mumbai and surrounding areas and its position in the Deccan volcanic stratigraphy, India. Journal of the Geological Society of India 53, 359–365.

Shannon, P.M., Moore, J.G., Jacob, A.W.B., Makris, J., 1993. Cretaceous and Tertiary basin development west of Ireland. In: Parker, J.R. (Ed.), Petroleum Geology of Northwest Europe: Proceedings of the 4th Conference. Geological Society, London, pp. 1057–1066.

Sharma, M., 1997. Siberian Traps. In: Mahoney, J.J., Coffin, M.F. (Eds.), Large Igneous Provinces: Continental, Oceanic, and Planetary Flood Volcanism. American Geophysical Union Monograph, vol. 100, pp. 273–295.

Sharp, W., Ludwig, K.R., Chadwick, O.A., Amundson, R., Glaser, L.L., 2003. Dating fluvial terraces by ^{230}Th/U on pedogenic carbonate, Wind River Basin, Wyoming. Quaternary Research 59, 139–150.

Sheth, H.C., 1999. Flood basalts and large igneous provinces from deep mantle plumes: fact, fiction and fallacy. Tectonophysics 311, 1–29.

Sheth, H.C., 2000. The timing of crustal extension, diking, and the eruption of the Deccan flood basalts. International Geological Review 42, 1007–1016.

Sheth, H.C., 2005. From Deccan to Reunion: No trace of a mantle plume. In: Foulger, G.R., Natland, J.H., Presnall, D.C., Anderson, D.L. (Eds.), Plates, Plumes and Paradigms. Special Paper, vol. 388. Geological Society of America, Boulder, Colorado, pp. 477–501.

Sheth, H.C., Chandrashekharam, D., 1997. Plume-rift interaction in the Deccan Province. Physics of the Earth and Planetary Interiors 99, 179–187.

Sheth, H.C., Pande, K., Bhutani, R., 2001. ^{40}Ar–^{39}Ar ages of Bombay trachytes: evidence for a Palaeocene phase of Deccan volcanism. Geophysical Research Letters 28, 3513–3516.

Simms, M.J., 2000. The sub-basaltic surface in northwest Ireland and its significance for interpreting the Tertiary history of the region. Proceedings of the Geological Association 111, 321–336.

Sleep, N.H., 1990. Hotspots and mantle plumes: some phenomology. Journal of Geophysical Research 95, 6715–6736.

Sleep, N.H., 1994. Lithospheric thinning by midplate mantle plumes and the thermal history of hot plume material ponded at sublithospheric depths. Journal of Geophysical Research 99, 9327–9343.

Sleep, N.H., 1996. Lateral flow of hot plume material ponded at sublithospheric depths. Journal of Geophysical Research 101, 28065–28083.

Sleep, N.H., 1997. Lateral flow and ponding of starting plume material. Journal of Geophysical Research 102, 10001–10012.

Smallwood, J.H., Gill, C.E., 2002. The rise and fall of the Faroes–Shetland Basin: evidence from seismic mapping of the Balder Formation. Journal of the Geological Society (London) 159, 627–630.

Smith, R.B., Braile, L.W., 1993. Topographic signature, space-time evolution, and physical properties of the Yellowstone–Snake River Plain volcanic system: the Yellowstone hotspot. In: Snoke, A.W., Steidtmann, J.R., Roberts, S.M. (Eds.), Geology of Wyoming: Geological Survey of Wyoming Memoir, vol. 5, pp. 694–754.

Spohn, T., Schubert, G., 1982. Convective thinning of the lithosphere: a mechanism for the initiation of continental rifting. Journal of Geophysical Research 87, 4669–4681.

Stewart, I.J., 1987. A revised stratigraphic interpretation of the Early Palaeogene of the central North Sea. In: Brooks, J., Glennie, K. (Eds.), Petroleum Geology of North West Europe. Graham and Trotman, London, pp. 557–576.

Suppe, J., Powell, C., Berry, R., 1975. Regional topography, seismicity, Quaternary volcanism, and the present-day tectonics of the western United States. American Journal of Science 275A, 397–436.

Surkov, V.S., 2002. Neogenean evolution of the young Ural–Siberian Platform. Russian Geology and Geophysics 43, 754–761.

Steinberger, B., 2000. Plumes in a convecting mantle: models and observations for individual hotspots. Journal of Geophysical Research 105, 11127–11152.

Takahahshi, E., Nakajima, K., Wright, T.L., 1998. Origin of the Columbia River basalts: melting model of a heterogeneous plume head. Earth and Planetary Science letters 162, 63–80.

Tandon, S.K., Sood, A., Andrews, J.E., Dennis, P.F., 1995. Paleoenvironments of the Dinosaur-Bearing Lameta Beds (Maastrichtian), Narmada Valley, central India. Palaeogeography, Palaeoclimatology, Palaeoecology 117, 153–184.

Taylor, D.W., Bright, R.C., 1987. Drainage history of the Bonneville Basin. In: Kopp, R.S., Cohenour, R.E. (Eds.), Cenozoic Geology of Western Utah: Utah Geological Association Publication, vol. 16, pp. 239–256.

Tanton, L.T., Hager, B.H., 2000. Melt intrusion as a trigger for lithospheric foundering and the eruption of the Siberian flood basalts. Geophysical Research Letters 27, 3937–3940.

Tiley, R., McKenzie, D.P., White, N.J., 2003. The elastic thickness of the British Isles. Journal of the Geological Society (London) 160, 499–502.

Thompson, R.N., Gibson, S.A., 1991. Subcontinental mantle plumes, hotspots and pre-existing thinspots. Journal of the Geological Society (London) 148, 973–977.

Todal, A., Eldholm, O., 1998. Continental margin of western India and Deccan large igneous province. Marine Geophysical Researches 20, 273–291.

Tolan, T.L., Reidel, S.P., Beeson, M.H., Anderson, J.L., Fecht, K.R., Swanson, D.A., 1989. Revisions of the extent and volume of the Columbia River Basalt Group. In: Reidel, S.P., Hooper, P.R. (Eds.), Volcanism and tectonism in the Columbia River Flood-Basalt Province. Geological Society of America Special Paper, vol. 2329, pp. 1–20.

Turcotte, D.L., Schubert, G., 2002. Geodynamics, 2nd edition. Cambridge University Press. 456 pp.

van Wijk, J.W., Huismans, R.S., ter Voorde, M., Cloetingh, S.A.P.L., 2001. Melt generation at volcanic continental margins: no need for a mantle plume? Geophysical Research Letters 28, 3995–3998.

Vogt, P.R., 1983. The Iceland Plume: status of the hypothesis after a decade of new work. In: Bott, M.P.H., et al. (Eds.), Structure and Development of the Greenland-Scotland Ridge. Plenum, New York, pp. 191–213.

Vyssotski, A.V., Vyssotski, V.N., Nezhdanov, A.A., 2006. Evolution of the West Siberian Basin. Marine and Petroleum Geology 23, 93–126.

Waite, G.P., Smith, R.B., 2002. Seismic evidence for fluid migration accompanying subsidence of the Yellowstone caldera. Journal of Geophysical Research 107, 2177. doi:10.1029/2001JB000586.

Waite, G.P., Smith, R.B., Allen, R.M., 2006. V–P and V–S structure of the Yellowstone Hotspot upper mantle from teleseismic tomography: